

MDPI

Article

Silversol[®] (a Colloidal Nanosilver Formulation) Inhibits Growth of Antibiotic-Resistant Staphylococcus aureus by Disrupting Its Physiology in Multiple Ways

Nidhi Thakkar ^{1,†}, Gemini Gajera ^{1,†}, Dilip Mehta ² and Vijay Kothari ^{1,*}

- Institute of Science, Nirma University, Ahmedabad 382481, India; 21ftphds68@nirmauni.ac.in (N.T.); 20ftphds55@nirmauni.ac.in (G.G.)
- ² Viridis BioPharma Pvt. Ltd., Mumbai 400043, India; dilipmehta39@hotmail.com
- * Correspondence: vijay.kothari@nirmauni.ac.in
- [†] These authors contributed equally to this work.

Abstract: Antibiotic-resistant strains of *Staphylococcus aureus* are being viewed as a serious threat by various public health agencies. Identifying novel targets in this important pathogen is crucial to the development of new effective antibacterial formulations. We investigated the antibacterial effect of a colloidal nanosilver formulation, Silversol[®], against an antibiotic-resistant strain of *S. aureus* using appropriate in vitro assays. Moreover, we deciphered the molecular mechanisms underlying this formulation's anti-*S. aureus* activity using whole transcriptome analysis. Lower concentrations of the test formulation exerted a bacteriostatic effect against this pathogen, and higher concentrations exerted a bactericidal effect. Silversol[®] at sub-lethal concentration was found to disturb multiple physiological traits of *S. aureus* such as growth, antibiotic susceptibility, membrane permeability, efflux, protein synthesis and export, biofilm and exopolysaccharide production, etc. Transcriptome data revealed that the genes coding for transcriptional regulators, efflux machinery, transferases, β -lactam resistance, oxidoreductases, metal homeostasis, virulence factors, and arginine biosynthesis are expressed differently under the influence of the test formulation. Genes (argG and argH) involved in arginine biosynthesis emerged among the major targets of Silversol[®] s antibacterial activity against *S. aureus*.

Keywords: antibiotic resistance; arginine biosynthesis; biofilm; efflux; membrane permeability; nanosilver; network analysis; transcriptome



Citation: Thakkar, N.; Gajera, G.; Mehta, D.; Kothari, V. Silversol® (a Colloidal Nanosilver Formulation) Inhibits Growth of Antibiotic-Resistant *Staphylococcus* aureus by Disrupting Its Physiology in Multiple Ways. *Pharmaceutics* 2024, 16, 726. https://doi.org/10.3390/

Academic Editors: Eva Torres-Sangiao and Erkko O. Ylösmäki

Received: 2 May 2024 Revised: 22 May 2024 Accepted: 24 May 2024 Published: 28 May 2024

pharmaceutics16060726



Copyright: © 2024 by the authors. Licensee MDPI, Basel, Switzerland. This article is an open access article distributed under the terms and conditions of the Creative Commons Attribution (CC BY) license (https://creativecommons.org/licenses/by/4.0/).

1. Introduction

Historically, silver has long been in use for various therapeutic purposes. It is an important ingredient of multiple traditional medicine formulations [1–3]. Modern times have also witnessed numerous reports [4–6] describing different types of biological activities of silver. Antimicrobial activity of different forms of silver against different groups of microorganisms has also been reported, e.g., antiviral [7–9], antibacterial [7,10,11], antifungal [12,13], antiprotozoal [14], and anthelmintic [15,16]. Different forms of silver (e.g., silver salts, metallic, or colloidal) may have different mechanisms of action and varying magnitudes of biological efficacy. The antibacterial potency of silver assumes importance in the face of the AMR (antimicrobial resistance) pandemic. A review of the literature did not provide strong indications of bacteria developing resistance against silver [17]. Silver is reported to exert its bactericidal activity by modulating cell membrane permeability, interrupting DNA replication, and inducing the generation of reactive oxygen species (ROS) [18–22]. However, a more detailed investigation is still required to reveal additional molecular mechanisms underlying the antibacterial activity of silver.

We chose a colloidal nanosilver solution as a test formulation for this study, as the metallic form of silver is believed to be more potent than its ionic counterpart [23]. Nanopar-

ticles are defined as particles of size < 100 nm [24], and nanoparticles of metals can be expected to score high on the parameter of bioavailability compared to larger particles of the same metal [25]. The potential of metal oxide nanocarriers for targeted drug delivery toward the treatment of infectious diseases and as biomedical materials has been nicely reviewed by Saha et al. [26] and Nikolova and Chavali [27], respectively. Due to their small size and larger surface area, nanoparticles show enhanced colloidal stability and, therefore, increased bioavailability.

The target pathogen for this study was an antibiotic-resistant strain of Staphylococcus aureus. This Gram-positive bacterium is amongst the few most well-known and versatile bacterial pathogens, whose antibiotic-resistant phenotypes are listed by various public health agencies like the World Health Organization (WHO; https://www.who.int/publications/ i/item/WHO-EMP-IAU-2017.12; accessed on 23 April 2024), Centers for Disease Control and Prevention (CDC; https://www.cdc.gov/drugresistance/biggest-threats.html; accessed on 19 April 2024), and the Indian government's Department of Biotechnology (DBT; https://dbtindia.gov.in/sites/default/files/IPPL_final.pdf; accessed on 29 March 2024); moreover, this bacterium is among the priority pathogens for which there is a pressing requirement to discover new antibacterial agents [28]. The present study examined the effect of Silversol® (a colloidal nanosilver formulation) on S. aureus's growth, various important phenotypic traits, and gene expression profile at the whole transcriptome level. Silversol already has a history of clinical use for the management of oral health [29], skin diseases, diabetic ulcers, burns, and wound care/wound disinfection (https://www.rxsilver.com/index_htm_files/ABLSilversafety.pdf; accessed on 29 March 2024). As S. aureus is one of the most common clinical isolates [30,31], we made an effort to gain insights into Silversol's antibacterial activity against this particular pathogen.

2. Materials and Methods

2.1. Colloidal Silver Formulation

The Silversol® test formulation (100 ppm; batch ID: V-Silwater22-47), originally formulated by American Biotech Labs (American Fork, UT, USA), was sourced from Viridis BioPharma Pvt. Ltd., Govandi Gaonthan, Mumbai, India. This colloidal silver mixture is documented to exert various biological effects [23]. It comprises zero-valent metallic silver particles in their elemental form that are covered in silver oxide. The manufacturer claims its particle size range to lie between 5 and 50 nm.

2.2. Bacterial Culture

The strain of *S. aureus* utilized in this study (ATCC 43300) was procured from HiMedia, Mumbai, India. Though this strain is claimed to be resistant to methicillin and oxacillin (https://www.atcc.org/products/43300; accessed on 1 March 2024), disc diffusion assay in our lab did yield a zone of inhibition of 26.5 ± 9.19 and 23 ± 7.07 mm surrounding methicillin and oxacillin discs (Table S1 and Figure S1). However, our transcriptome of this strain, conducted as a part of this study, showed this strain to be positive for expression of the *mecA* gene, whose presence is considered a defining characteristic for labeling *S. aureus* as methicillin-resistant [32]. Antibiogram of this strain generated in our lab showed it to be resistant to four macrolide antibiotics (erythromycin, clindamycin, azithromycin, and clarithromycin), and intermediate to amoxicillin/clavulanic acid. To characterize the test strain in terms of virulence, we challenged the nematode worm *Caenorhabditis elegans* with it (OD₇₆₄ = 1.50), and it was able to kill 100% of worms within 24 h (Figure S2). In summary, the *S. aureus* strain used in this study can be said to possess the traits of antibiotic resistance and virulence.

This bacterium was maintained on Tryptone soy agar (HiMedia) slants. For the purpose of different assays described in this report, (unless described otherwise) it was grown in tryptone soy broth (pH 7.0 \pm 0.2; HiMedia) for 24 \pm 1 h at 35 °C. Inoculum was standardized as OD₆₂₅ between 0.08–0.10 (at par with McFarland turbidity standard 0.5).

Pharmaceutics **2024**, 16, 726 3 of 27

2.3. Growth Inhibition Assay

The effect of Silversol on bacterial growth was assessed using a broth dilution assay. *S. aureus* was inoculated (at $10\% \ v/v$) in tryptone soy broth with or without Silversol (0.1–60 ppm), followed by incubation at 35 °C for 24 ± 1 h. The total volume of the system was 2 mL in 15 mL test tubes. Random intermittent shaking was provided during incubation. At the end of incubation, cell density was measured as A_{764} (Agilent Cary 60 UV–Vis; Agilent, Santa Clara, CA, USA).

The minimum concentration of Silversol inhibiting \geq 80% growth was considered as the minimum inhibitory concentration (MIC) [33]. From each of the tubes with no visible growth, 0.1 mL of culture broth was spread on tryptone soy agar plates. These agar plates were inspected for the appearance of bacterial colonies during a 72 h incubation (at 35 °C) to determine the minimum bactericidal concentration (MBC). Extended incubation for a total of 72 h was practiced to enable differentiation of the genuine bactericidal effect from any possible post-antibiotic effect [34,35]. The minimum concentration of Silversol, capable of inhibiting the appearance of bacterial growth on agar surfaces almost completely, was considered as the MBC. Vancomycin was used as a positive control.

The growth curve of the test bacterium in the absence and presence of Silversol (at the sub-MIC level) was also generated, wherein incubation was carried out under continuous shaking (120 rpm).

2.4. Antibiotic Susceptibility Assay

Antibiogram of Silversol pre-exposed-S. aureus was obtained using a disc diffusion assay performed in accordance with the Clinical and Laboratory Standards Institute (CLSI) guidelines [36] and was compared with that of the control culture (which received no Silversol pre-exposure). S. aureus was grown in tryptone soy broth, with or without Silversol. Following overnight incubation (24 \pm 1 h), 1 mL of culture broth was used for cell density quantification at 764 nm, and cells from the remaining 1 mL culture were pelleted down using centrifugation (10 min at $13,600 \times g$). The pellet thus obtained was then resuspended in 1 mL of phosphate buffer (HiMedia; pH 7.0 ± 0.2), followed by centrifugation. The resulting cell pellet was utilized to prepare the inoculum for the subsequent disc diffusion assay by resuspending it in normal saline. The OD₆₂₅ of the inoculum was adjusted to range from 0.08-0.10 to achieve equivalence to McFarland turbidity standard 0.5. The known volume (0.1 mL) of this inoculum was then spread onto cation-adjusted Muller-Hinton agar (HiMedia) in 150 mm plates (Borosil, Mumbai, India), followed by loading antibiotic discs (Icosa G-I PLUS; HiMedia, Mumbai, India) onto the agar surface. The plates were then incubated at 35 °C for 18 ± 1 h, followed by the observation and measurement of the diameter of the zone of inhibition.

2.5. Biofilm Assay

Biofilm formation is an important virulence trait, and hence the effect of Silversol on the biofilm-forming ability of *S. aureus*, as well as on pre-formed biofilm was investigated using four different biofilm assays using the methodology described in our previous publication [37]. A flowchart illustrating all the biofilm assays is provided in Figure 1, wherein biofilm quantification was carried out using crystal violet assay [38], and biofilm viability assessment was conducted using MTT assay [39]. Vancomycin at the sub-MIC level (3 ppm) was used as a positive control.

For the crystal violet assay, the biofilm-containing tubes (after discarding the inside liquid) were subjected to washing with phosphate buffer saline (PBS) to remove all the non-adhering planktonic bacteria and then air-dried for fifteen minutes. Then, each of the washed tubes was subjected to staining with 2 mL of 0.4% aqueous crystal violet (Central Drug House, Delhi, India) for thirty minutes. Each tube was then washed twice with sterile distilled water (2 mL), followed by immediate de-staining with 2 mL of 95% ethanol. After allowing de-staining for 45 min, 1 mL of de-staining solution was transferred into separate tubes, and A_{580} was measured (Agilent Cary 60 UV–Vis; Agilent, Santa Clara, CA, USA).

Pharmaceutics **2024**, 16, 726 4 of 27

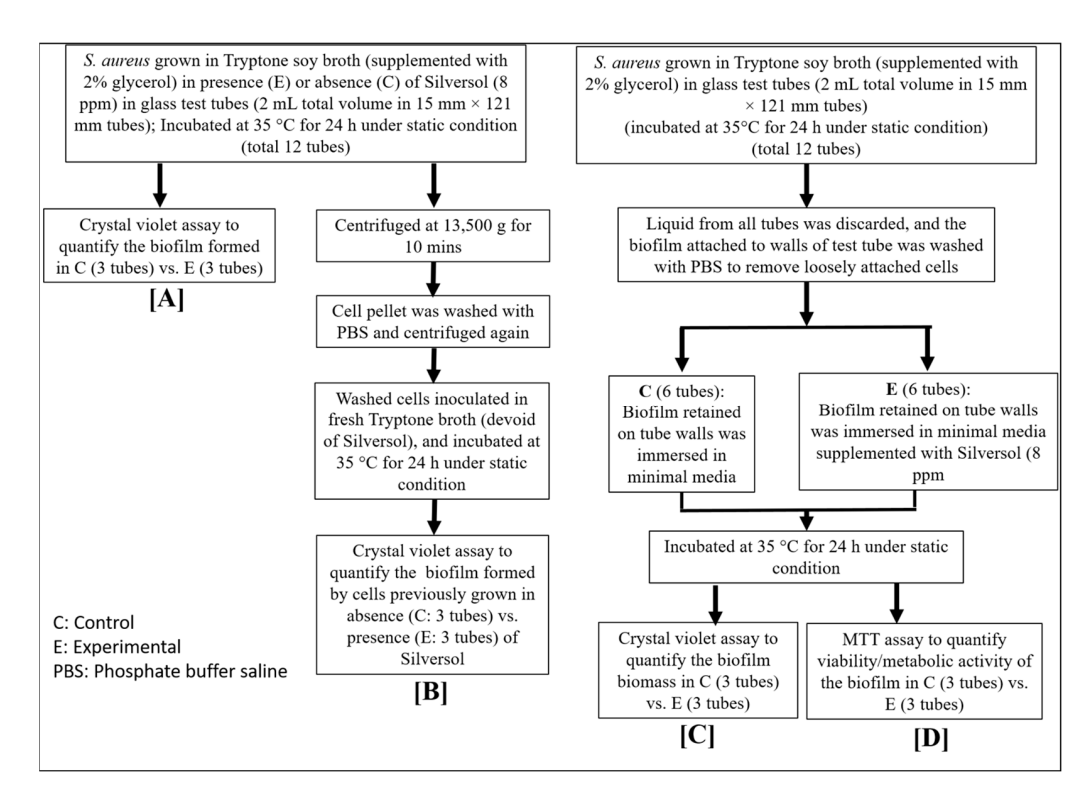


Figure 1. Flowchart depicting schematic of all biofilm assays. (**A**) Quantification of biofilm formation in the presence or absence of Silversol; (**B**) quantification of biofilm formation by silver-pre-treated vs. non-pre-treated *S. aureus* cells; (**C**) quantification of biofilm eradication after adding Silversol onto pre-formed biofilm; and (**D**) quantification of Silversol's effect on metabolic activity of pre-formed biofilm.

For the MTT assay, the tubes containing biofilm (after discarding the inside liquid content) were washed with PBS to remove all the non-adherent bacteria, and then air-dried for fifteen minutes. Then, 1.8 mL of minimal media (NaCl 1 g/L, K₂HPO₄ 5 g/L, MgSO₄ 0.1 g/L, NH₄Cl 2 g/L, sucrose 15 g/L, yeast extract 0.1 g/L, pH 7.4 \pm 0.2) was added into each tube, followed by addition of 200 μ L of 0.3% MTT [3-(4,5-Dimethylthiazol-2-yl)-2,5-iphenyltetrazolium Bromide; HiMedia]. Following a 24 h incubation at 35 °C, all liquid was discarded, and the remaining purple formazan derivatives were dissolved in 2 mL of DMSO, and then A₅₄₀ was measured.

2.6. Exopolysaccharide (EPS) Quantification

S.~aureus was grown in 20 mL of tryptone soy broth contained in 100 mL flasks (containing or not containing Silversol). Incubation was provided at 35 °C for 24 \pm 1 h under static conditions with intermittent shaking. At the end of incubation, cell density was quantified as OD_{764} . For EPS quantification [40], the culture broth was centrifuged (13,600×g; 10 min). To the resulting supernatant, chilled acetone (Merck, Mumbai, India) was added in a 1:2 ratio and allowed to rest for 30 min for the EPS to precipitate. Thus, the precipitated EPS was then separated out by filtration using pre-weighed Whatman #1 filter paper (Whatman International Ltd., Buckinghamshire, UK). Filter paper containing EPS was then dried for 24 h, and the weight of the EPS on the paper was calculated.

2.7. Efflux Assay

An ethidium bromide (EtBr) efflux assay with *S. aureus* was performed using the method described in [41]. *S. aureus* cells, grown overnight in tryptone soy broth medium, were loaded with 8 ppm of EtBr (HiMedia) in the presence of 75 ppm of reserpine (HiMedia; positive control) or Silversol (8 ppm). Any effective efflux inhibitor like reserpine will inhibit efflux during this loading step. Cells were incubated at 35 $^{\circ}$ C for 20 min and then pelleted by centrifugation (13,600× g; 10 min). The medium was decanted, and the cell pellet

Pharmaceutics **2024**, 16, 726 5 of 27

was resuspended in fresh tryptone soy broth medium, either with or without Silversol (8 ppm), to an optical density of $OD_{764} = 0.20$. The EtBr efflux was then determined by quantification of fluorescence at excitation and emission wavelengths of 530 and 600 nm in a spectrofluorometer (JASCO FP-6500; Jasco International Co. Ltd., Tokyo, Japan).

2.8. Protein Estimation

The extracellular protein present in the bacterial culture (grown in the presence or absence of Silversol) supernatant, and intracellular protein in the cell lysate was quantified using the Folin–Lowry method [42,43]. After measuring cell density, 1 mL of *S. aureus* culture was centrifuged (13,600×g), and the resulting supernatant liquid was utilized for extracellular protein estimation. The left cell pellet was subjected to lysis [44] for the release of intracellular proteins. Briefly, the cell pellet was subjected to washing with phosphate buffer (pH 7.4) and centrifugation (13,600×g). The resulting pellet was then reconstituted in 1 mL of chilled lysis buffer (0.1 g of sodium dodecyl sulfate, 0.5 g of sodium deoxycholate, 0.60 g of Tris HCl, 0.876 g of NaCl, and 1 mL of Triton X-100, in 99 mL of distilled water) and centrifuged (500 rpm) for 30 min at 4 °C to provide agitation. This was followed by another round of low-temp (4 °C) centrifugation (13,600×g) for 20 min. The resulting cell lysate (i.e., supernatant) was utilized for protein estimation.

2.9. Membrane Permeability Assay

A propidium iodide (PI) uptake assay [45,46] was performed to quantify membrane permeability. *S. aureus* cells grown overnight in tryptone soy broth were centrifuged, and the cell pellet was dissolved in PBS to attain $OD_{764} = 1.50 \pm 0.05$. This cell suspension was exposed to Silversol (8 ppm) for 30 min at 35 °C in an incubator. The negative control contained cells with no Silversol exposure. After incubation, 2 ml of each test sample was centrifuged at $13,600 \times g$. The resulting pellet was washed with PBS, resuspended in PBS, and then PI (Invitrogen, Mumbai, India) at a final concentration of 10 ppm was added into the suspension. This mixture was kept in the dark for 10 min, followed by quantification of fluorescence, employing 544 nm as excitation and 612 as emission wavelength, using a spectrofluorometer (JASCO FP-6500). Triton-X (final concentration $0.5\% \ v/v$) was kept as a positive control.

2.10. Transcriptome Analysis

To unravel the molecular mechanisms through which Silversol inhibited bacterial growth and modulated various physiological traits, the gene expression pattern of *S. aureus* challenged with the sub-MIC level of Silversol (8 ppm) was compared with that of the control culture at the whole transcriptome scale. The overall workflow of this whole transcriptome analysis (WTA) aimed at capturing a holistic picture regarding modes of action of the test formulation is given in Figure S3.

2.10.1. RNA Extraction

Bacterial RNA was extracted by the Trizol (Invitrogen Bioservices, Mumbai, India; 343909) method. Precipitation was achieved by isopropanol followed by washing with ethanol (75%), and RNA was then dissolved in nuclease-free water. The extracted RNA was quantified on a Qubit 4.0 fluorometer (Thermofisher, Mumbai, India; Q33238) employing an RNA HS assay kit (Thermofisher; Q32851) as per the manufacturer's protocol. The concentration and purity of RNA were assessed using Nanodrop 1000. Finally, the RIN (RNA Integrity Number) value was determined by checking the RNA on the TapeStation using HS RNA ScreenTape (Agilent) (Table S2).

2.10.2. Library Preparation

Final libraries were quantified using a Qubit 4.0 fluorometer (Thermofisher; Q33238) using a DNA HS assay kit (Thermofisher; Q32851). To determine the insert size of the library, it was queried on Tapestation 4150 (Agilent) using highly sensitive D1000 screentapes (Agilent; 5067-5582). The acquired sizes of all libraries are given in Table S2.

Pharmaceutics **2024**, 16, 726 6 of 27

2.10.3. Genome Annotation and Functional Analysis

Quality assessment of the raw fastq reads of the sample was achieved using FastQC v.0.11.9 (default parameters) [47]. The raw fastq reads were pre-processed using Fastp v.0.20.1 [48], followed by a reassessment of the quality using FastQC.

The *S. aureus* genome (GCA_000006765.1_ASM676v1) was indexed using bowtie2-build [49] v2.4.2 (default parameters). The processed reads were mapped to the indexed *S. aureus* genome using bowtie2 v2.4.2 parameters. The aligned reads from each of the samples were quantified using feature count v. 0.46. 1 [50] to determine the gene counts. Gene counts thus obtained were then fed as inputs to edgeR [51] using an exact test (parameters: dispersion 0.1) for estimation of differential expression. The down- and upregulated sequences were acquired from the *S. aureus* coding file and fed into blast2go [52] for annotation to generate the gene ontology (GO) terms. Latter terms were then processed using the Wego [53] tool to create gene ontology bar plots.

All the raw sequence data were submitted to the Sequence Read Archive. The relevant accession number is SRX15156375 (https://www.ncbi.nlm.nih.gov/sra/SRX15156375; accessed on 20 January 2024).

2.11. Network Analysis

From among all the differentially expressed genes (DEGs) in Silversol-exposed S. aureus, those fulfilling the dual filter criteria of False Discovery Rate (FDR) ≤ 0.05 and log fold change ≥ 2 were selected for further network analysis. A list of such DEGs was input into the STRING (v.11.5) database [54] to create the PPI (Protein–Protein Interaction) network. Members of this PPI network were then arranged in descending order of 'node degree' (a quantitative indication of connectivity with other proteins or genes), and those above a specified threshold value were forwarded for ranking by the cytoHubba plugin (v.3.9.1) [55] of Cytoscape [56]. As cytoHubba uses twelve different ranking methods, we considered the DEGs to be top-ranked by a minimum of 6 different methods (50% of the total ranking methods) for further investigation. These top-ranked proteins were then shortlisted for local cluster analysis using STRING, and those that were part of multiple clusters were labeled as potential 'hubs' to be investigated for additional validation of their targetability. The term 'hub' refers to a protein or gene interacting with multiple other proteins/genes. These identified hubs were then subjected to co-occurrence analysis across genomes of multiple pathogens to visualize whether an antibacterial agent targeting these hubs is likely to exert a broad-spectrum activity. The above-described sequence of operations enabled us to end up with a limited number of proteins fulfilling multiple biological and statistical significance criteria simultaneously: (i) FDR \leq 0.05; (ii) log fold change \geq 2; (iii) relatively higher node degree; (iv) top-ranking by a minimum of 6 cytoHubba methods; and (v) member of >1 local network cluster.

2.12. Polymerase Chain Reaction (RT-PCR)

Differential expression of the potential hubs found using network analysis of DEGs revealed from WTA was further confirmed using PCR. Primer designing for the shortlisted genes was carried out using Primer3 Plus [57]. These primer sequences were checked for their binding exclusivity to the target gene sequence within the whole *S. aureus* genome. Primer sequences for these target genes are given in Table 1. RNA extraction and quality checks were carried out in the same way as described in the preceding section. cDNA synthesis was carried out using the synthesis kit SuperScriptTM VILOTM (Invitrogen Biosciences). PCR assay employed the gene-specific primers purchased from Sigma-Aldrich. *rpsU* was run as the endogenous control gene. FastStart Essential DNA Green Master mix (Roche, Darmstadt, Germany; 06402712001) was used as the reaction mix. The real-time PCR assay was performed on a QuantStudio 5 real-time PCR machine (Thermo Fisher Scientific, Waltham, MA, USA). The temperature profile followed is given in Table S3.

Table 1. Primer sequences for the target genes.

Gene ID/Name	Gene ID/Name Primers					
argG (DA471_RS02560)	FP: 5'-TCAAAACCTATGGGGCAGAG-3' RP: 5'-TTCCGATACCATGCTTACCA-3'	233				
argH (DA471_RS02555)	FP: 5'-TGCAACTATGCTTGCGAATC-3' RP: 5'-TGCAACTTACCACCAGCATC-3'	189				
rpsU (DA471_RS07645) (Control gene)	FP: 5'-AATGAATCACTTGAAGATGCGTTA-3' RP: 5'-TTTGAATTTACGTTTACGTGCAG-3'	150				

2.13. Statistics

All results reported are means of three or more independent experiments, each performed in triplicate. Statistical significance was assessed using a t-test performed using Microsoft Excel® (Version 2108), and data with $p \le 0.05$ were considered to be significant.

3. Results and Discussion

3.1. Growth Inhibitory Effect of Silversol against S. aureus Follows a Non-Linear Dose–Response Pattern

Silversol exerted its growth inhibitory effect against *S. aureus* at concentrations \geq 5 ppm (Figure 2A). Interestingly, the dose–response curve assumed different shapes over different concentration ranges (Figure 2A, inset box), considering 'inhibition of growth' as the 'response'. For example, in the 1–10 ppm range, it followed a pattern following the threshold model, wherein 5 ppm was the minimum concentration required to generate the response. In the 7–15 ppm range, it assumed an 'inverted U' shape, while in the 10–25 ppm range, it assumed a 'U' shape. These different patterns of dose-response relationship can be appreciated better by looking at relevant explanations in [58,59], etc. The non-linear nature of this dose–response curve stemmed from the fact that some of the higher concentrations (15–20 ppm) were less effective at inhibiting bacterial growth than some of the lower concentrations (8–10 ppm) (Supplementary Materials, Figure S4). Such paradoxical antibacterial effect of bactericidal substances, often referred to as the 'Eagle Effect', has been reported in previous literature too, with *S. aureus* as well as other bacteria. As early as 1948, Eagle and Musselman [60] reported an in vitro paradoxical effect of penicillin against S. aureus and streptococci. Here, the paradox is that a decrease was observed, instead of an increase, in bactericidal activity at concentrations exceeding the MBC. A similar paradoxical effect was also observed in the case of S. aureus challenged with cefotaxime [61]. Such observations were also reported in studies investigating the recovery of bacteria from the toxic effects of penicillin [62]. Streptococcus faecalis and Group B hemolytic streptococci exposed briefly to higher concentrations of penicillin were reported to require less time to recover from the toxic effects of penicillin than when they were exposed to lower concentrations for an equal duration. Penicillin at the dose level of 200 mg/kg given to mice infected with Group B beta-hemolytic streptococci killed the pathogen more slowly than the lower dose of 3 mg/kg [63]. Though over the decades, there have been numerous reports of anomalous drug activity where the usual direct relationship between concentration of antibacterial compounds and inhibition of bacterial growth is not followed, detailed mechanistic explanations for such non-linear responses have not yet penetrated the conventional microbiology wisdom. Further, all such cases of a non-linear dose–response relationship cannot be explained by any single concept, e.g., 'Eagle effect', 'hormesis', or any other such term. While it is most likely that further such examples will continue to appear in the literature, as and when discovered, wider reporting and acceptance of such 'unusual' observations across the microbiological community is desired, and so are the efforts to unravel the underlying mechanistic details. One possible explanation for such non-linear responses may be that the bacteria exhibit a hormetic response in order to enhance their resilience when encountered with subinhibitory concentrations of antibacterial formulations or any

Pharmaceutics **2024**, 16, 726 8 of 27

other stressors [59]. Since these responses have been reported with multiple bacteria and different antibiotics [64–67], hormesis can be viewed as a generalized adaptive mechanism implemented by bacteria to strengthen their resistance against antibiotics. Adoption of such defensive responses may be driven by the ability of low doses of antibacterial substances to modulate the transcriptional activity of bacteria.

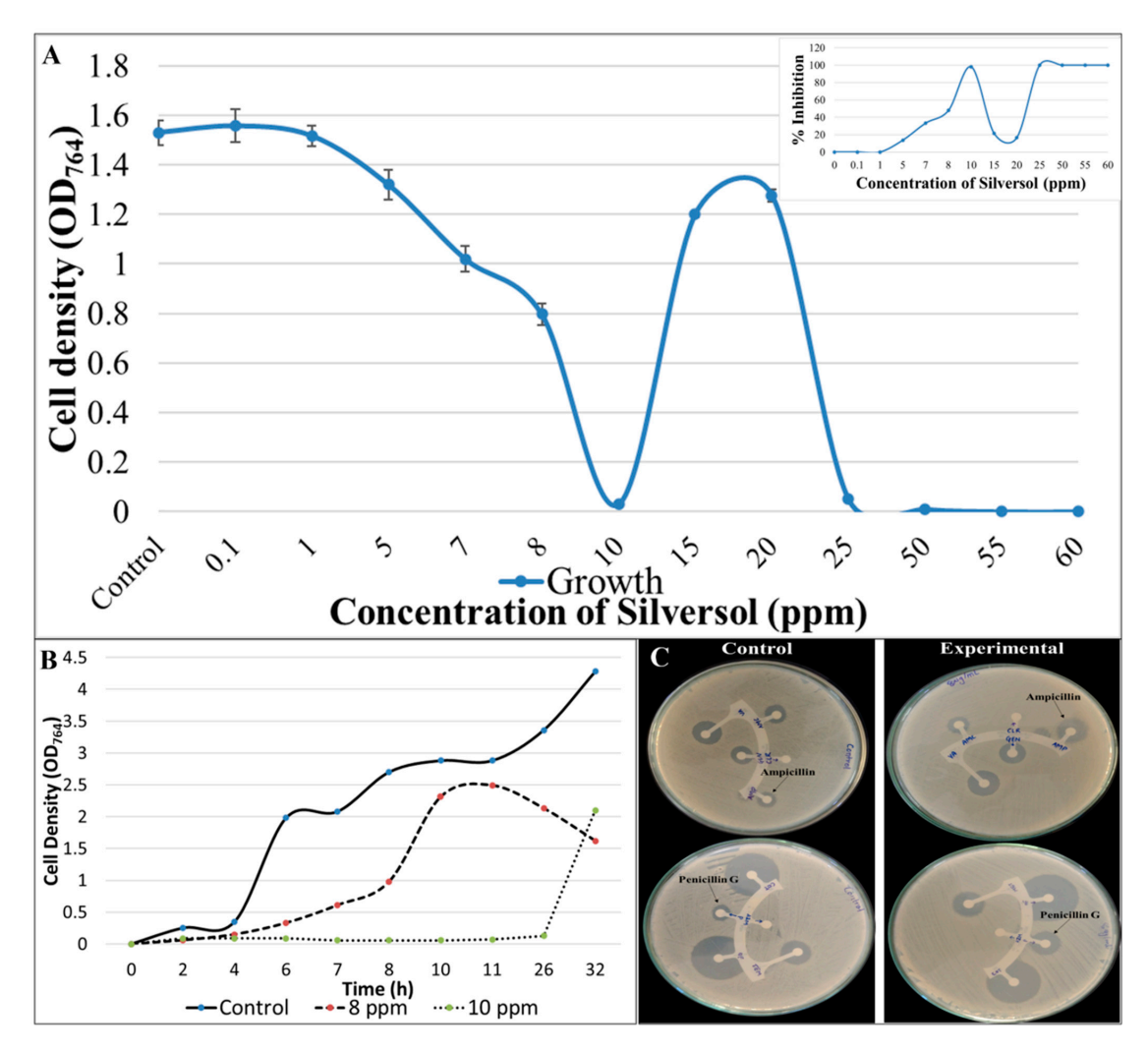


Figure 2. Silversol inhibits the growth of *S. aureus* and enhances its susceptibility toward β-lactams. (**A**) Silversol inhibits the growth of *S. aureus*. Bacterial growth was measured as OD_{764} . Vancomycin (5 μg/mL) employed as the positive control inhibited bacterial growth by 100%. All the OD points plotted differed from the control at p < 0.01. The inset box shows the plotted percent inhibition vs. time for a better idea of the shape of the dose–response curve. (**B**) Growth curve of *S. aureus* in the presence or absence of Silversol. *S. aureus* could achieve a lesser growth rate and cell density in the presence of bacteriostatic concentrations of Silversol. (**C**) Silversol-pre-treatment enhances bacterial susceptibility to beta-lactam antibiotics. Silversol-pre-treated cells (experimental panel) can be seen surrounded by larger zones of inhibition encircling discs of penicillin and ampicillin.

The minimum concentration of Silversol required to achieve complete visible inhibition of bacterial growth was 10 ppm, and hence it can be considered as the MIC. However, the growth-inhibitory effect of Silversol up to 25 ppm can largely be said to be bacteriostatic, as the cells exposed to these concentrations when plated on fresh media (devoid of Silversol) were able to give rise to lawn growth (Figure S5). Concentrations of Silversol \geq 50 ppm exerted a bactericidal effect, and the cells exposed to these concentrations when plated on fresh media (devoid of Silversol) could give rise only to a few isolated colonies. Based on observation of those plates, 60 ppm can be considered as the MBC. Non-cidal action

Pharmaceutics **2024**, 16, 726 9 of 27

of Silversol at lower concentrations was also confirmed in the growth curve experiment, wherein the bacterium was able to partially overcome the growth-inhibitory effect of Silversol if allowed extended incubation (Figure 2B). However, the maximum cell density achieved by *S. aureus* in the presence of 8 ppm and 10 ppm Silversol was 1.71 and 2.03-fold less than that of the control. The onset of growth was much delayed in the presence of 10 ppm Silversol. While the control culture was still in the exponential phase of growth at the 32nd hour of incubation, the death phase had already started in the experimental culture (8 ppm Silversol) by the 26th hour.

Silversol's 8 ppm level was found to inhibit the growth of *S. aureus* by nearly 50%, and hence considering this as \sim IC₅₀, all further experiments (unless specified otherwise) were conducted at this concentration.

3.2. Silversol Pre-Treatment Renders S. aureus More Susceptible to Ampicillin and Penicillin G

When Silversol-pre-treated *S. aureus* cells were subjected to antibiotic susceptibility assay using the disc diffusion method, their susceptibility to ampicillin and penicillin was increased by approximately 1.5-fold (Table 2; Figure 2C). To nullify any possible role of the 'post-antibiotic effect', we confirmed that Silversol-pre-treated cells grow at the same rate as that of the control when transferred into fresh media (devoid of silver). This resistance-modifying activity of Silversol becomes important in light of the fact that strains of *S. aureus* exhibiting beta-lactam resistance have established a considerable ecological niche among human pathogens [68]. As approximately only 10% of *S. aureus* clinical isolates (in the United States) are susceptible to penicillin (https://www.cdc.gov/hai/settings/lab/lab_mrsa.html; accessed on 3 January 2024), resistance modifiers making the bacteria more susceptible to one or more beta-lactams can help widen the utility spectrum of classical antibiotics.

Table 2. Staphylococcus aureus challenged with antibiotics following pre-treatment with Silversol.

Antibiotic	Concentration (µg) –	Diameter of Zone	Diameter of Zone of Inhibition (mm)			
Antibiotic	Concentration (µg) –	Control	Experimental	- % Difference		
Penicillin G	10	14 ± 1.14	20.5 ± 2.12	46.42 **		
Oxacillin	1	23 ± 7.07	25.5 ± 6.36			
Erythromycin	15	R	R	_		
Clindamycin	2	R	R	_		
Linezolid	30	29.5 ± 3.53	30 ± 2.12	_		
Co-trimoxazole	25	35 ± 0	35 ± 0	_		
Vancomycin	30	20.5 ± 2.12	20 ± 0.70	_		
Tetracycline	30	29 ± 1.14	31 ± 1.41	— Non-significant		
Chloramphenicol	30	28 ± 1.41	28 ± 1.41	_		
Gentamicin	10	23 ± 12.02	23.5 ± 9.19	_		
Azithromycin	15	R	R	_		
Ofloxacin	5	35 ± 0	36 ± 1.41	_		
Methicillin	5	26.5 ± 9.19	23.5 ± 4.94	_		
Amoxycillin/clavulanic acid	30	14 ± 0	16 ± 2.82	_		
Clarithromycin	15	R	R	_		
Ampicillin	10	14 ± 1.41	21.5 ± 2.12	53.57 *		
Amikacin	30	22.5 ± 2.12	23 ± 2.82			
Cephalothin	30	30 ± 7.07	31 ± 5.65	_ Non-significant		
Novobiocin	5	36 ± 1.41	36 ± 1.41	Ton organicum		
Teicoplanin	10	21 ± 1.41	21.5 ± 0.70	_		

An antibiogram of the test strain was generated using the antibiotic discs-Icosa G-I Plus (HiMedia, Mumbai, India) by performing a disc diffusion assay in line with the CLSI guidelines. R: resistant, i.e., no zone of inhibition was observed. * $p \le 0.05$, ** $p \le 0.01$.

3.3. Silversol Inhibits Biofilm Formation and Renders Pre-Formed Biofilm Non-Viable

S. aureus in the presence of non-growth inhibitory concentration of Silversol could form 59% less biofilm than the control cells. Neither pre-treatment with Silversol could compromise the bacterial ability to form biofilm, nor could Silversol eradicate pre-formed biofilm. However, Silversol brought down the biofilm viability to zero when added to pre-formed biofilm (Figure 3A). These results indicate that Silversol could penetrate the biofilm matrix to exert its effect on the metabolic activity/viability of constituent cells. Reduced biofilm formation and decrease in biofilm viability in the presence of Silversol was also previously reported by us in the case of *Pseudomonas aeruginosa* [37]. This anti-biofilm activity of Silversol is important considering that bacterial biofilms exert antibiotic tolerance at higher levels, and biofilm infections are more difficult to treat [69]. Nanoparticles of antibacterial preparations have been demonstrated to possess notable efficacy against bacterial biofilms in a variety of bacterial species [70], and the results of the present study corroborate with the same. The anti-biofilm activity of Silversol can be one of the attributes of this formulation, making it effective at wound disinfection as biofilm-infected wounds take longer to heal [71] in the absence of an efficient anti-biofilm therapy.

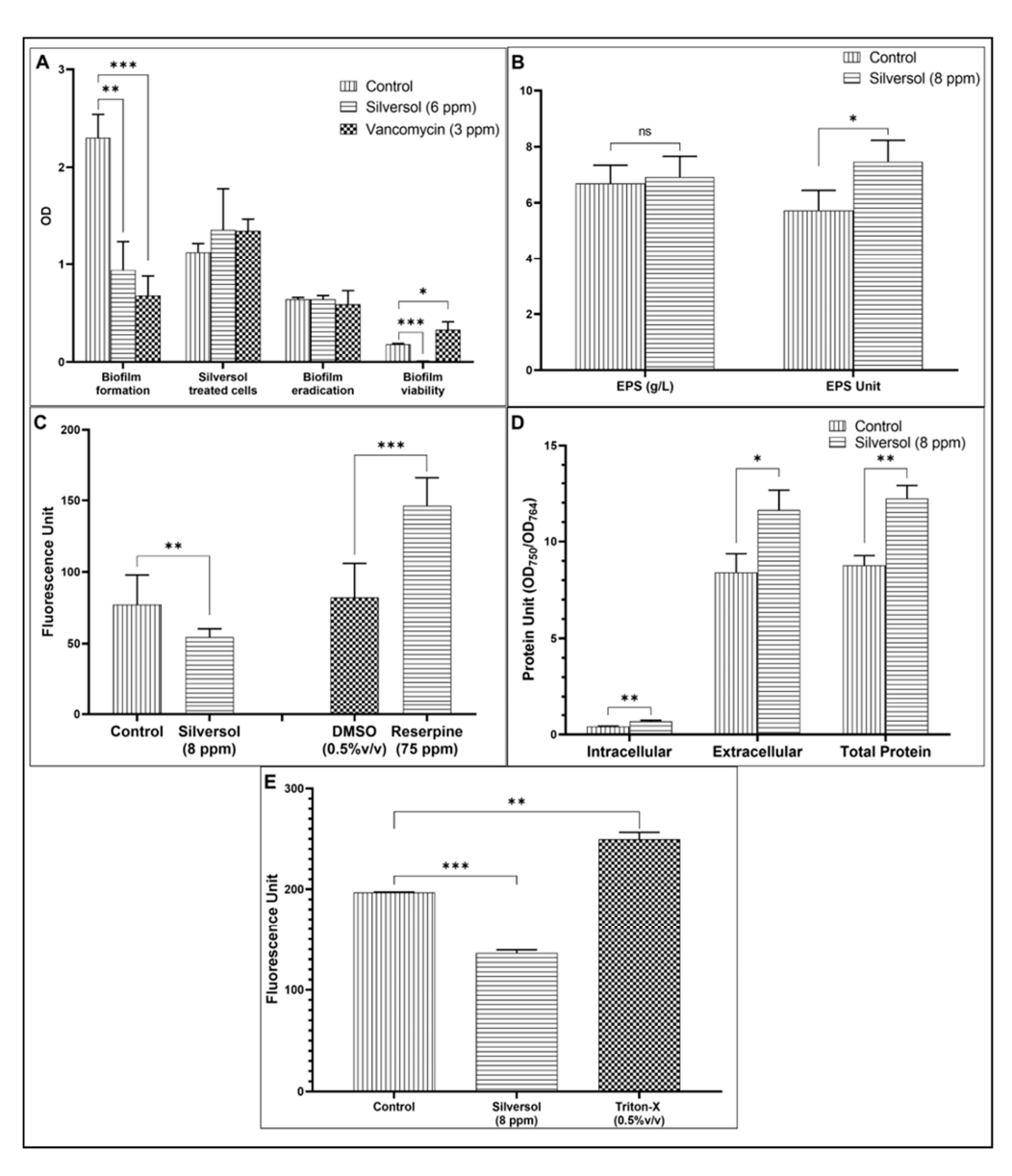


Figure 3. Silversol modulates various important physiological and phenotypic traits in *S. aureus*. (**A**) Silversol inhibits biofilm formation in *S. aureus* and renders pre-formed biofilm metabolically inactive

The non-inhibitory concentration of Silversol allowed S. aureus to form a lesser biofilm (first group of bars); Silversol-pre-treated cells formed biofilm at par to the control cells; when Silversol was added onto pre-formed biofilm, it was not able to eradicate it (third group of bars), but reduced its metabolic activity to a non-detectable level (fourth group of bars). Vancomycin employed as a positive control at the sub-MIC level inhibited growth by 26% \pm 0.12 and biofilm formation by 70% \pm 12.22. Vancomycin did not eradicate biofilm when added to pre-formed biofilm, but it increased its metabolic activity by $83\% \pm 30.8$. While biofilm formation was quantified using crystal violet assay, biofilm viability was estimated using MTT assay. (B) Silversol enhances exopolysaccharide (EPS) synthesis in S. aureus. Though Silversol-supplemented media contained a lesser number of bacterial cells, they produced EPS in an amount at par with their Silversol-unexposed counterparts (first group of bars). However, when the EPS Unit was calculated as the cell density (OD₇₆₄): EPS (g/L) ratio, this was found to be $30\% \pm 6$ higher in the presence of Silversol. (C) Silversol triggers overexpression of efflux machinery in S. aureus. Fluorescence of the intracellularly accumulated EtBr was $29\% \pm 5.77$ lesser in Silversol-exposed S. aureus. Higher (78% \pm 20.12) intracellular accumulation of EtBr was observed in the presence of the known efflux inhibitor, reserpine. (D) S. aureus grown in the presence of Silversol exhibited higher protein synthesis and secretion. Extracellular and intracellular protein concentrations in S. aureus grown in the presence of Silversol at the sub-MIC level were significantly higher (38% \pm 13.9 and 61 \pm 12.7%, respectively) compared to its Silversol-non-exposed counterpart. Protein Unit (ratio of protein concentration: cell density) was calculated to rule out any effect of cell density on protein synthesis. (E) Silversol exposure reduces the membrane permeability of S. aureus. Silversol-pre-exposed cells allowed 30% \pm 3.18 lesser propidium iodide (PI) to enter them. Cells pre-exposed to Triton-X, a known disruptor of bacterial membranes, allowed 26% \pm 6.97 more PI to enter, as indicated by the fluorescence of intracellularly accumulated dye. * $p \le 0.05$, ** $p \le 0.01$, *** $p \le 0.001$; ns: not significant.

3.4. Silversol Makes S. aureus Synthesize and Secrete More Exopolysaccharide (EPS)

EPS is an important component of the biofilm matrix, and it enables the bacterial pathogen to effectively adhere to the host and colonize there [72,73]. The EPS matrix can also protect the pathogen from a variety of challenges including host defense factors [74]. Silversol-pre-exposed *S. aureus* culture had a 1.30-fold higher EPS production (Figure 3B). Enhanced EPS secretion may be taken as a response to the stress induced in the bacterial population by Silversol, as EPS production is known to be a part of the bacterial stress response [75,76].

3.5. Silversol Triggers Overexpression of Efflux Machinery in S. aureus

S. aureus cells accumulated lesser EtBr when incubated with Silversol than when in Silversol-free media (Figure 3C). This lesser intracellular accumulation of EtBr can be said to have resulted from overexpression of efflux machinery in Silversol-exposed *S. aureus*. While efflux pumps play an important role in detoxification, their overexpression may have a negative effect on bacterial physiology [77], as overactive efflux machinery will export even some of the essential intracellular content. The results of this in vitro efflux assay corroborate well with the overexpression of efflux-associated genes (*terC* and *mepA*) in Silversol-exposed *S. aureus* described later.

3.6. Protein Synthesis and Export in S. aureus Is Enhanced in the Presence of Silversol

Extracellular and intracellular protein content in *S. aureus* culture grown in the presence of Silversol was found to be 1.38-fold and 1.61-fold higher, respectively, than the control (Figure 3D). This indicates that not only was overall protein synthesis increased but also its export was increased under the influence of Silversol. This increased protein export may have arisen from compromised membrane integrity and/or overexpression of efflux machinery [78–80]. Bacteria might be responding to the inhibitory effect of such antimicrobials acting as suppressors of protein synthesis by elevating their protein synthesis

sis and/or secretion machinery to compensate for the inhibitory effect of the antibacterial substances [81]. Such up-regulation of protein synthesis can be believed to have originated from the translational reprogramming in the stressed bacterial cells [82] while they deal with the stress of Silversol's antibacterial effect.

3.7. Silversol Alters Membrane Permeability of S. aureus

The membrane permeability of bacterial cells was quantified in terms of their ability to uptake the fluorescent dye propidium iodide. Lesser uptake of this dye by bacterial cells in the presence of Silversol indicates this formulation's ability to alter membrane permeability (Figure 3E). Reduced permeability might have compromised bacterial capacity to allow intake of nutrients leading to stunted growth. This combined with overexpression of efflux function (Figure 3C) and protein secretion (Figure 3D) can be expected to force bacteria to face a scarcity of essential nutrients and metabolites. Alterations in membrane functioning can affect multiple bacterial traits such as surface charge, permeability, fluidity, stability of the bacterial membrane, antibiotic susceptibility, etc. [83]. A correlation between the antibacterial activity of Silversol and its ability to alter membrane fluidity cannot be ruled out, as expected of other membranotropic agents [84].

3.8. Silversol Causes Multiple Genes in S. aureus to Express Differentially

After confirming the growth-inhibitory activity of Silversol against *S. aureus*, we compared the gene expression profile of the Silversol-exposed *S. aureus* with that of the control at the whole transcriptome level. Whole transcriptome analysis identified a total of 90 differentially expressed genes (3.32% of the total genome) in Silversol-treated *S. aureus*, of which 49 were down-regulated (Table 3) and 41 were up-regulated (Table 4). The corresponding heat map (Figure S6) and volcano plot (Figure S7) are provided in the Supplementary Materials. A summary of function-wise categorization of all the differentially expressed genes (DEGs) is presented in Figure 4.

Among the down-regulated DEGs, the one with the highest log fold change (logFC 5.14) value was *CidR*, which is the transcriptional regulator of the LysR family. This regulator is known to control stationary phase cell death in *S. aureus* [85] by influencing the expression of operons that display pro- and anti-death functions. Since the primary role of CidR regulon is to limit acetate-dependent potentiation of cell death in staphylococcal populations, its down-regulation can be expected to have a negative effect on bacterial growth. Besides regulating stationary-phase survival of *S. aureus*, the *CidR* gene also affects antibiotic tolerance in this bacterium [86].

Table 3. List of down-regulated genes in Silversol-exposed *S. aureus* satisfying the dual criteria of log fold change \geq 2 and FDR \leq 0.05.

Sr. No.	Feature ID	Gene	Product/Function	Log FC	FDR	Node Degree
1	DA471_RS06440	CidR	LysR family transcriptional regulator	5.14	1.39×10^{-6}	NA
2	DA471_RS06435	leuA	LeuA family protein	4	0.0003	1
3	DA471_RS09790	-	DUF1270 domain-containing protein	3.69	0.0003	NA
4	DA471_RS02560	argG	Argininosuccinate synthase	3.28	0.002	7
5	DA471_RS11145	Spa	Staphylococcal protein A	3.26	0.002	NA
6	DA471_RS02555	argH	Argininosuccinate lyase	3.15	0.002	5
7	DA471_RS02685	-	Minor capsid protein	3.08	0.017	NA
8	DA471_RS06430	tsaC	L-threonylcarbamoyladenylate synthase	2.99	0.006	NA
9	DA471_RS13755	arcD	Arginine-ornithine antiporter	2.96	0.004	4
10	DA471_RS01680	ctnA	ABC transporter permease subunit	2.91	0.005	NA
11	DA471_RS11020	isdA	LPXTG cell wall anchor domain-containing protein	2.89	0.005	0

 Table 3. Cont.

Sr. No.	Feature ID	Gene	Log FC	FDR	Node Degree	
12	DA471_RS01245	-	Hypothetical protein	2.88	0.005	NA
13	DA471_RS03325	тар	MAP domain-containing protein	2.84	0.006	0
14	DA471_RS09785	-	DUF771 domain-containing protein	2.84	0.006	NA
15	DA471_RS09780	-	Hypothetical protein	2.79	0.007	NA
16	DA471_RS09775	-	DUF739 family protein	2.78	0.007	NA
17	DA471_RS01255	traH	Conjugal transfer protein	2.73	0.008	NA
18	DA471_RS01250	-	Hypothetical protein	2.73	0.008	NA
19	DA471_RS05905	pfkB	Fructosamine kinase family protein	2.73	0.008	0
20	DA471_RS01275	-	Hypothetical protein	2.7	0.009	NA
21	DA471_RS13750	argF	Ornithine carbamoyltransferase	2.69	0.009	9
22	DA471_RS13375	immR	Helix-turn-helix domain-containing protein	2.66	0.009	0
23	DA471_RS05395	-	Hypothetical protein	2.65	0.009	0
24	DA471_RS06160	kdpB	K ⁺ -transporting ATPase subunit B	2.64	0.01	2
25	DA471_RS01260	RepB	Replication initiation factor domain-containing protein	2.62	0.01	0
26	DA471_RS06165	kdpA	Potassium-transporting ATPase subunit KdpA	2.62	0.01	2
27	DA471_RS13765	arcR	Crp/Fnr family transcriptional regulator	2.58	0.01	4
28	DA471_RS06155	kdpC	K ⁺ -transporting ATPase subunit C	2.57	0.01	2
29	DA471_RS13745	arcA	Arginine deiminase	2.55	0.01	6
30	DA471_RS00130	thrS	Threonine tRNA ligase	2.54	0.01	1
31	DA471_RS13125	mecA	PBP2a family beta-lactam-resistant peptidoglycan transpeptidase MecA	2.49	0.02	0
32	DA471_RS11175	Yxep2	M20 family metallopeptidase	2.46	0.02	NA
33	DA471_RS13760	arcC	Carbamate kinase	2.46	0.02	6
34	DA471_RS10170	blaZ	Penicillin-hydrolyzing class A beta-lactamase BlaZ	2.42	0.02	0
35	DA471_RS01675	glnQ	Amino acid ABC transporter ATP-binding protein	2.41	0.02	NA
36	DA471_RS08555	-	Aminotransferase class I/II-fold pyridoxal phosphate-dependent enzyme	2.41	0.03	NA
37	DA471_RS05580	ldhD	D-lactate dehydrogenase	2.34	0.03	NA
38	DA471_RS06060	nrdG	Anaerobic ribonucleoside–triphosphate reductase-activating protein	2.32	0.03	0
39	DA471_RS09810	RecT	Recombinase RecT	2.32	0.03	NA
40	DA471_RS09795	-	DUF1108 family protein	2.3	0.03	NA
41	DA471_RS13995	-	Terminase small subunit	2.28	0.03	0
42	DA471_RS09805	-	AAA family ATPase	2.27	0.03	0
43	DA471_RS00250	uspA	Universal stress protein	2.24	0.04	NA
44	DA471_RS09265	-	Lactococcin 972 family bacteriocin	2.19	0.04	NA
45	DA471_RS06295	fmtB	LPXTG-anchored DUF1542 repeat protein FmtB	2.19	0.05	NA
46	DA471_RS09840		Hypothetical protein	2.18	0.05	NA
47	DA471_RS04505	yghA	SDR family oxidoreductase	2.17	0.05	NA
48	DA471_RS10350	ftnA	H-type ferritin FtnA	2.17	0.05	0
49	DA471_RS01240	NTPase	ATP-binding protein	2.15	0.05	0

NA: not applicable, as STIRING did not include these genes in the PPI network.

Table 4. List of up-regulated genes in Silversol-treated *S. aureus* fulfilling the dual criteria of log fold change \geq 2 and FDR \leq 0.05.

Sr. No.	Feature ID Gene Product/Function				FDR	Node Degree	
1	DA471_RS04350	-	Hypothetical protein	3.68	0.0003	NA	
2	DA471_RS05495	-	FUSC family protein	3.46	0.0007	0	
3	DA471_RS00585	-	Proline dehydrogenase	3.45	0.0007	1	
4	DA471_RS07140	-	Hypothetical protein	3.43	0.003	NA	
5	DA471_RS04685	hrtB	ABC transporter permease	3.15	0.002	NA	
6	DA471_RS06605	pyrC	Dihydroorotase	3.14	0.002	5	
7	DA471_RS00725	-	Hypothetical protein	3.08	0.003	NA	
8	DA471_RS04680	hrtA	ABC transporter ATP-binding protein	3.07	0.003	NA	
9	DA471_RS06600	carA	Carbamoyl phosphate synthase small subunit	2.97	0.004	7	
10	DA471_RS11535	-	Hypothetical protein	2.93	0.006	NA	
11	DA471_RS13920	cspC	Cold-shock protein	2.93	0.005	NA	
12	DA471_RS06615	pyrP	Uracil permease	2.92	0.005	NA	
13	DA471_RS06595	carB	Carbamoyl-phosphate synthase large subunit	2.83	0.006	8	
14	DA471_RS06590	pyrF	Orotidine-5'-phosphate decarboxylase	2.78	0.007	4	
15	DA471_RS08840	brnQ	Branched-chain amino acid transport system II carrier protein	2.69	0.009	0	
16	DA471_RS04800	YbgA	YbgA family protein	2.68	0.009	NA	
17	DA471_RS12105	CvpA	CvpA family protein	2.65	0.009	0	
18	DA471_RS05490	-	DUF2188 domain-containing protein	2.63	0.01	NA	
19	DA471_RS11425	TerC	TerC family protein	2.63	0.01	NA	
20	DA471_RS02540	rocD	Ornithine-oxo-acid transaminase	2.63	0.01	3	
21	DA471_RS14065	-	Helix-turn-helix domain-containing protein	2.62	0.01	0	
22	DA471_RS13410	vraE	Peptide resistance ABC transporter permease subunit VraE	2.6	0.01	NA	
23	DA471_RS05980	pheP	Amino acid permease	2.54	0.01	NA	
24	DA471_RS08680	терА	Multidrug efflux MATE transporter MepA	2.46	0.02	0	
25	DA471_RS10850	aldA	Aldehyde dehydrogenase family protein	2.45	0.02	0	
26	DA471_RS05800	ssaA1	CHAP domain-containing protein	2.44	0.02	NA	
27	DA471_RS06585	pyrE	Orotate phosphoribosyltransferase	2.44	0.02	5	
28	DA471_RS03355	-	Aldo/keto reductase	2.44	0.02	NA	
29	DA471_RS13415	vraD	Peptide resistance ABC transporter ATP-binding subunit VraD	2.36	0.03	NA	
30	DA471_RS12555	vraC	Protein VraC	2.33	0.03	NA	
31	DA471_RS00355	serA	Phosphoglycerate dehydrogenase	2.31	0.03	0	
32	DA471_RS00920	xerC	Tyrosine recombinase XerC	2.3	0.03	0	
33	DA471_RS06690	treP	PTS system trehalose-specific EIIBC component	2.3	0.03	0	
34	DA471_RS08610	-	DUF1398 family protein	2.28	0.03	NA	
35	DA471_RS03440	opuD2	BCCT family transporter	2.27	0.03	NA	
36	DA471_RS10560	-	Hypothetical protein	2.25	0.04	NA	
37	DA471_RS12545	vraA	AMP-binding protein	2.23	0.04	NA	
38	DA471_RS13380	Cspa	Cold-shock protein	2.22	0.04	0	
39	DA471_RS12915	-	Hypothetical protein	2.2	0.05	NA	
40	DA471_RS02880	acnA	Aconitate hydratase AcnA	2.18	0.05	0	
41	DA471_RS05505	DedA	DedA family protein	2.16	0.05	NA	

NA: not applicable, as STIRING did not include these genes in the PPI network. Genes in Tables 3 and 4 are arranged in descending order of fold change. The databases referred for gene functions are as follows: KEGG (Kyoto Encyclopedia of Genes and Genomes: https://www.genome.jp/kegg/; accessed on 1 January 2024); NCBI gene database (https://www.ncbi.nlm.nih.gov/nuccore/NC_002516; accessed on 1 January 2024); and Uniprot (https://www.uniprot.org/; accessed on 1 January 2024).

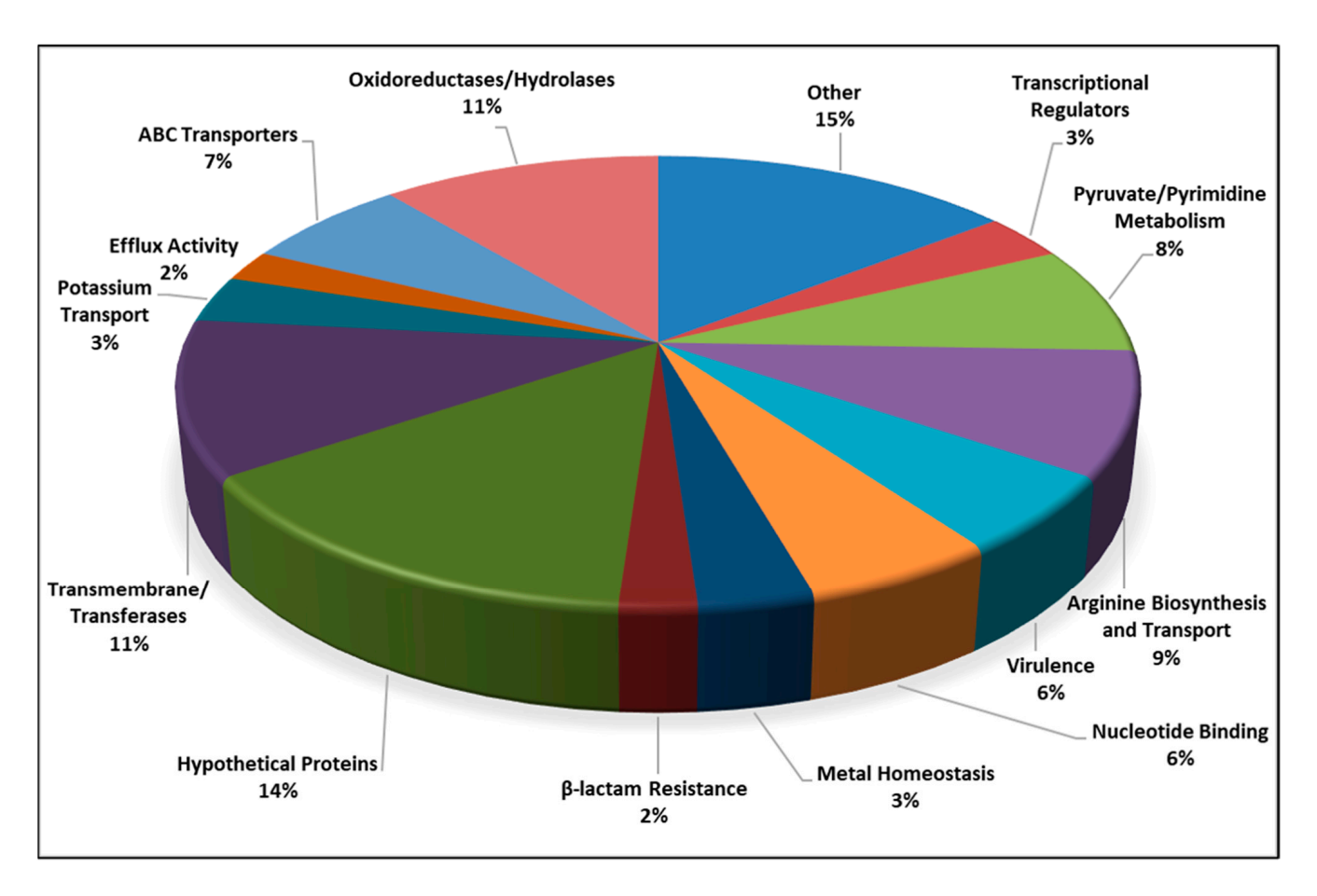


Figure 4. Function-wise categorization of the significantly differentially expressed genes in Silversol-treated *Staphylococcus aureus* (% values represent the fraction of the total number of DEGs).

Another heavily down-regulated gene in the Silversol-exposed *S. aureus* was *spa* (3.26\$) coding for staphylococcal protein A. The latter is a multifunctional virulence factor of *S. aureus*, which plays a role in the inhibition of the host innate and adaptive immune responses. Owing to its immunoglobulin-binding capacity, this protein confers protection on *S. aureus* from phagocytic killing via inhibition of the Ig Fc region. Additionally, the spa is known to prevent the host-elicited B-cell response, decrease long-term antibody production, inhibit osteogenesis, and act as a pro-inflammatory factor in the lung [87]. Protein A has also been identified as an essential component of the *S. aureus* biofilm, which induces bacterial aggregation in liquid medium and during biofilm formation. Besides interacting with multiple immunologically important eukaryotic receptors, protein A contributes considerably toward the development of biofilm-associated infections [88], and hence its down-regulation by Silversol can be of high clinical relevance.

In addition to the spa, other virulence-associated genes down-regulated in Silversol-exposed S. aureus were TraH (2.73 \downarrow) and the one coding for ABC transporter permease subunit (2.91 \downarrow). The latter is a part of the ABC transporter complex CntABCDF involved in the uptake of metal, particularly in the import of divalent metal ions like nickel, cobalt, and zinc. Its down-regulation may be expected to disturb metal homeostasis in bacterial populations as many important enzymes rely on their metal cofactors for proper functioning. This permease is also believed to contribute toward the virulence of S. aureus, as it has been shown to be necessary for full urease activity in vitro [89], and urease is well recognized as a virulence factor in multiple pathogenic bacteria [90–92].

TraH mentioned in the preceding paragraph is a conjugal transfer protein and a component of the Type IV secretion system (T4SS). Since for many Gram-positive pathogens, conjugative plasmid transfer is an important means of spreading antibiotic resistance,

components of T4SS are being viewed as potential targets for alternative anti-pathogenic strategies [93].

Among other important gene clusters down-regulated in Silversol-exposed *S. aureus*, one notable cluster was the kdp system, which is a potassium uptake system. Three components [kdpA $(2.62\downarrow)$, kdpB $(2.64\downarrow)$, and kdpC $(2.57\downarrow)$] of this system were found to be significantly down-regulated in our experimental culture. *kdpB* has been shown to be one of the core genes regulating cell death in *S. aureus* [94]. Potassium has many key functions within bacterial cells. For example, it is required for the activity of multiple intracellular enzymes, acts as an intracellular second messenger, and is involved in the maintenance of a constant internal pH and membrane potential. One of the clinically important characteristics of *S. aureus* is its ability to survive in/on high-salt areas of human nares and skin is also helped by its capacity for efficient potassium uptake and intracellular accumulation of this cation [95]. Since the kdp system is widely distributed among bacteria [96], any formulation targeting this system can be expected to exert a broad-spectrum antibacterial activity, and in fact, silver nanoparticles have been demonstrated to possess a broad activity spectrum in terms of their ability to inhibit the growth of different Gram-positive and Gram-negative bacteria [97,98].

Down-regulation of two of the genes, mecA and blaZ, associated with beta-lactam resistance corroborated well with results of antibiotic susceptibility (Figure 2C and Table 2), wherein Silversol-pre-exposure was found to increase the susceptibility of S. aureus to beta-lactams. The occurrence of mecA and blaZ genes has been reported in methicillin-resistant S. aureus associated with vaginitis among pregnant women [99]. Expression of these genes may be considered important for the expression of antibiotic-resistant phenotypes in clinical isolates, as the functionality of at least one mecA regulator is necessary for S. aureus to be oxacillin-resistant [100]. Penicillin resistance in S. aureus is manifested predominantly via the production of β -lactamase encoded by the blaZ gene, and testing for the presence of this gene is also recommended by the Clinical and Laboratory Standards Institute for cases of serious S. aureus infection [101].

Among the top ten up-regulated genes in Silversol-exposed S. aureus, two were hrtA $(3.07\uparrow)$ and hrtB $(3.15\uparrow)$. Four more genes (vraA, vraC, vraD, and vraE) coding for components of the ABC transporter complex hrt were also up-regulated. The HrtAB system is a hemin-regulated ABC transporter that protects S. aureus against hemin toxicity. Since S. aureus has been reported to launch an altered gene expression program involving differential expression of Hrt genes, when it senses membrane damage; differential up-regulation of hrtA and hrtB in our experimental culture can be taken as an indication of Silversol's ability to alter membrane permeability in this bacterium. Overexpression of hrtB can lead to dysregulated pore formation, and its up-regulation has also been reported in S. aureus challenged with channel-forming antimicrobial peptides [102]. The altered abundance of Hrt proteins has also been reported in *S. aureus* cultures facing alterations in iron status [103], and hence up-regulation of these genes in the presence of Silversol can be considered an indication of this formulation's ability to disturb iron homeostasis. Silversol's potential ability to trigger iron starvation in *S. aureus* can be one of the reasons underlying its successful clinical applications (e.g., wound disinfection), as the role of bacterial iron acquisition during pathogenesis is well established [104,105].

Among the top 25 up-regulated genes in Silversol-exposed S. aureus, two $[terC (2.63\uparrow)]$ and $mepA (2.46\uparrow)]$ were associated with efflux activity. Efflux machinery, besides throwing out toxic items, also has important physiological functions in bacteria [77]. In general, the up-regulation of efflux machinery can be taken as a sign of the bacteria making efforts for detoxification; for example, in the case of this study, they may be trying to efflux silver. However, overexpression of efflux function can lead to leakage of even essential molecules from within the cell, thereby negatively affecting bacterial growth and fitness. The way efflux inhibitors are considered potential anti-pathogenic agents [106], efflux agonists triggering overexpression of the efflux pumps can also be pursued as a novel antibacterial strategy. Of the two up-regulated genes mentioned above, TerC belongs to a family

of integral membrane proteins and has been implicated in resistance to metal ions like tellurium [107] and Mn [108]. TerC helps bacteria alleviate metal toxicity by participating in the efflux of metal ions. In the case of the present study, TerC might have been activated in response to silver overload. Owing to the widespread occurrence of the TerC family proteins among bacteria and its possible influence on host–pathogen interactions, it can be an important antibacterial target [109,110]. Another efflux-associated up-regulated gene *mepA* is a multidrug resistance efflux protein involved in transporting several clinically relevant monovalent and divalent biocides, the fluoroquinolone antibiotics, norfloxacin and ciprofloxacin, and also tigecycline [111]. Since mepA has a broad substrate profile [112], its poorly regulated overexpression (as observed in Silversol-exposed *S. aureus*) can trigger the efflux of multiple substrates, probably including some essential metabolites. Though metal nanoparticles have been postulated to exert inhibitory action against multidrug resistance efflux pumps [113], their ability to trigger uncontrolled overexpression also needs to be investigated for possible clinical exploitation.

3.9. Network Analysis of DEGs

To gain deeper insight into the interactions among DEGs identified in Silversolexposed S. aureus, we subjected all the DEGs to network analysis using STRING. The resulting Protein-Protein Interaction (PPI) (Figure 5A) network had 41 nodes connected through 41 edges, with an average node degree of 2. Since the number of edges (41) in this PPI network is almost 3.4-fold higher than expected (12), this network can be believed to possess a significantly higher number of interactions among the member proteins than what can be expected for a random set of proteins having similar sample size and degree distribution. Such an enrichment is indicative of the member proteins being biologically connected, at least partially. When all the 41 nodes were arranged in descending order of node degree, 22 nodes appeared to have a non-zero score, and we shortlisted the top 13 genes (Tables 3 and 4) with a node degree \geq 3 to be forwarded for ranking by different cytoHubba methods (Table 5). Then, we checked for genes that were among the top-ranked candidates by ≥ 6 cytoHubba methods. This enabled the shortlisting of six genes, which were ranked among the top six by ≥ 9 cytoHubba methods to be subjected to further cluster analysis. The interaction map of these six important genes (Figure 5B) revealed them to be networked with an average node degree score of 4.33. The number of edges in this network was 13 compared to the expected 1, for any such random set of proteins. The six genes were distributed among three different local network clusters. Two of the genes, argG and argH, were part of two of these three clusters, hence we chose them for further RT-PCR validation. PCR assay did confirm the differential expression of these two genes in Silversol-exposed S. aureus (Figure 6A). Hence, arginine metabolism can be believed to be one of the major targets of Silversol in S. aureus.

Arginine has an important role as a substituent for potassium. Under conditions of potassium limitation, bacteria respond by overproduction of arginine, which may partially substitute for potassium to buffer the negative charge of DNA [116]. However, in the presence of Silversol, *S. aureus* seems to have failed to do so, as in our study, the Silversol-exposed *S. aureus* is simultaneously suffering from potassium-limitation as well as downregulation of arginine biosynthesis.

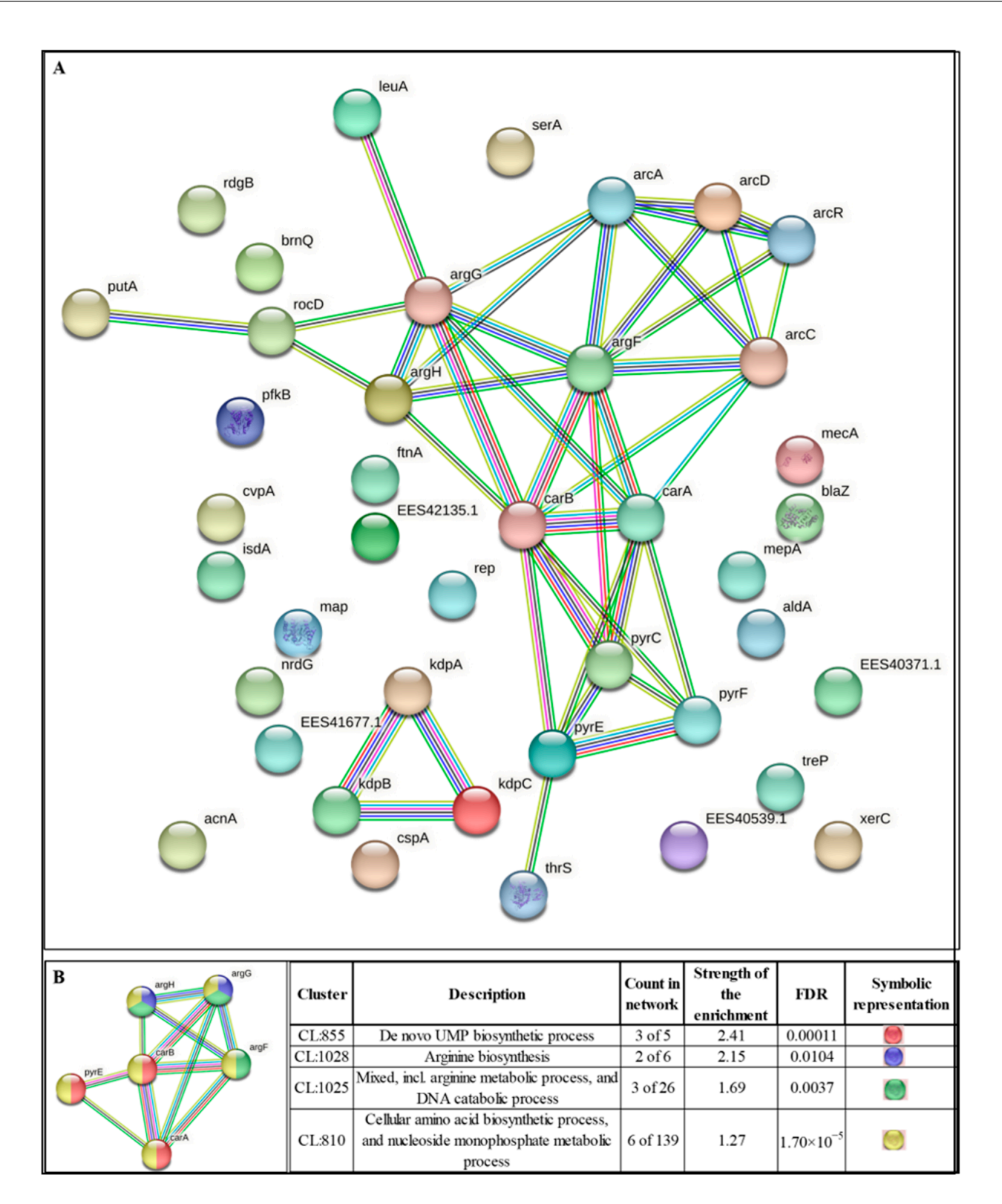


Figure 5. (**A**) Protein–Protein Interaction (PPI) network of DEGs following the dual criteria of fold change $\geq \log 2$ and FDR ≤ 0.05 in Silversol-exposed *S. aureus*. PPI enrichment *p*-value 3.81×10^{-11} . (**B**) PPI network of top-ranked genes shortlisted using cytoHubba among DEGs in Silversol-treated *S. aureus*. PPI enrichment *p*-value 1.81×10^{-14} .

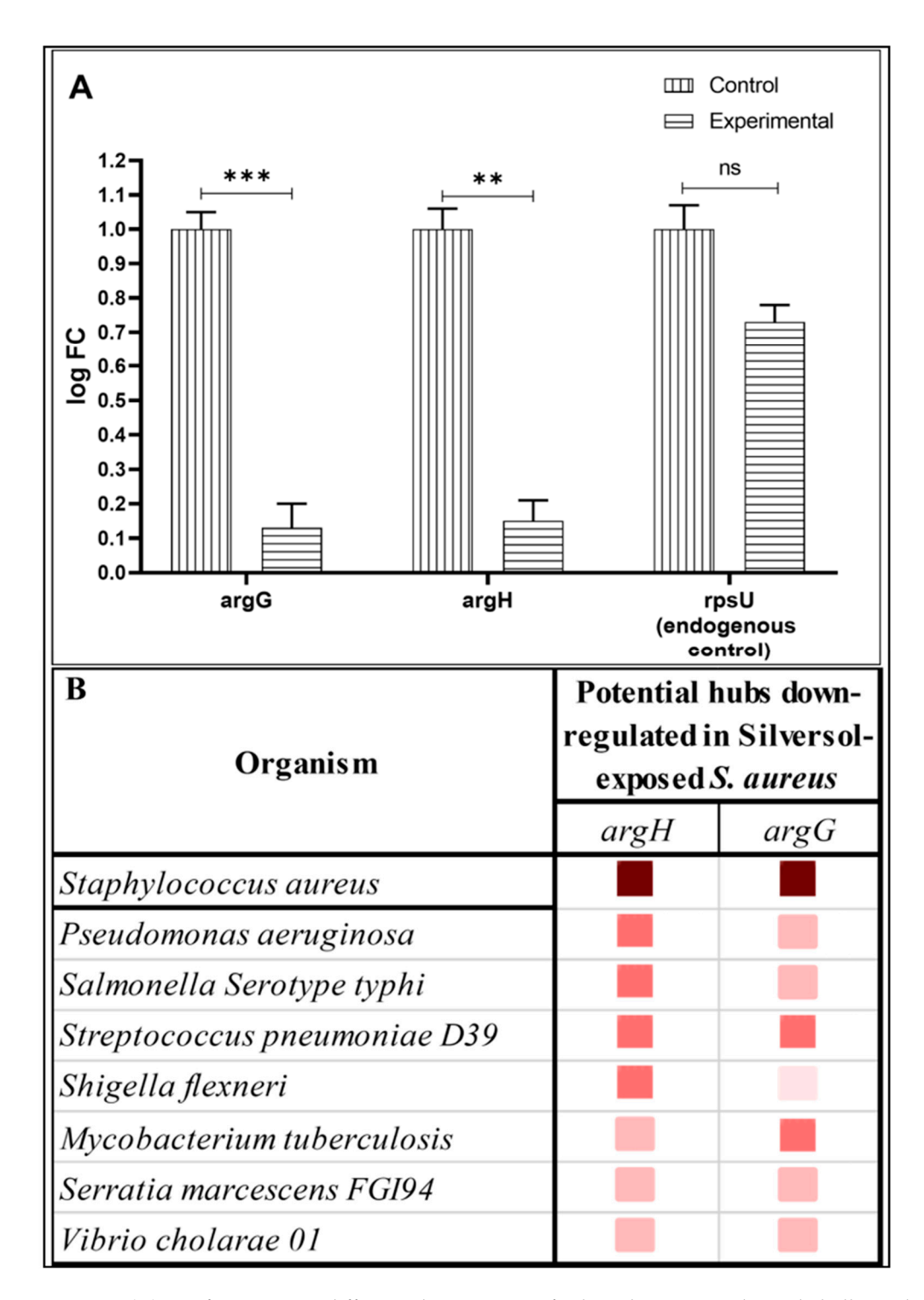


Figure 6. (A) Confirmation on differential expression of selected genes in Silversol-challenged *S. aureus* using RT-PCR. ** $p \le 0.01$, *** $p \le 0.001$, ns: not significant **(B)** Co-occurrence analysis of genes coding for potential targets in *S. aureus*, across multiple pathogens. The darker the shade of the squares, the higher the homology between the genes being compared.

Pharmaceutics **2024**, 16, 726 20 of 27

Table 5. CytoHubba ranking of the top twelve high node degree genes.

			Number of	Names of 12 Ranking Methods of CytoHubba and Rank Score Provided by Them											
No.	Gene ID Name	0	Degree	MNC	DMNC	MCC	Bottleneck	Eccentricity	Closeness	Radiality	Betweenness	Stress	SS	EPC	
1	1200	carA	11	8	8	0.466	66	1	0.5	9.5	3.090	9.810	38	0.57	8.39
2	0956	argG	10	6	6	0.475	36	1	0.5	8.5	2.909	4.335	22	0.67	7.79
3	0955	argH	10	7	7	0.439	42	1	0.5	9	3	9.933	34	0.57	8.21
4	1201	carB	10	9	9	0.405	68	2	0.5	10	3.181	20.516	60	0.47	8.49
5	1165	argF	9	8	8	0.437	50	5	0.5	9.5	3.090	13.885	44	0.53	8.48
6	1203	pyrE	9	5	5	0.518	30	1	0.5	8	2.818	1.598	8	0.8	7.39
7	1199	pyrC	3	5	5	0.518	30	1	0.5	8	2.818	1.598	8	0.8	7.40
8	2906	arcA	2	5	5	0.324	10	1	0.33	7.833	2.727	4.523	16	0.5	7.45
9	2903	arcC2	2	5	5	0.388	12	1	0.5	8	2.818	3.216	14	0.8	7.63
10	2902	arcR	2	3	3	0.308	4	1	0.33	6.833	2.545	0.581	4	0.67	5.93
11	1202	pyrF	2	4	4	0.568	24	1	0.33	7.166	2.545	0	0	1	6.88
12	0170	rocD	2	3	3	0.463	6	1	0.33	6.666	2.454	0	0	1	6.32

arcD, one of the high node degree genes, was not considered by cytoHubba.

All the six identified hubs were shown by cluster analysis to belong to amino acid biosynthesis (Figure 5B). Moreover, all six genes are participants in the arginine biosynthesis pathway. Three of them (*argG*, *argH*, and *argF*) are involved in the urea cycle, which is a part of the arginine biosynthesis pathway. Hence, amino acid metabolism in general, and arginine metabolism and urea cycle in particular, seem to be targeted by Silversol in *S. aureus*.

To provide increased confidence in our finding that one of the major modes of action of Silversol against *S. aureus* is to interfere with arginine synthesis, we conducted an additional experiment wherein S. aureus was incubated either in Silversol- or L-arginine (HiMedia)supplemented media, as well as in a media containing both Silversol and arginine together. Arginine supplementation allowed bacteria to overcome the inhibitory effect of Silversol (Figure 7), confirming Silversol's ability to interfere with arginine metabolism. This observation becomes relevant in the context that amino acid pathways have recently been targeted as a novel approach to managing bacterial infections. In particular, arginine metabolism has been illustrated to be important for bacterial pathogenesis [114]. Since arginine and its metabolites are utilized as energy sources by various pathogens, its reduced availability can trigger nutrient stress. Reduced availability of arginine may also lead to reduced expression of various pathogenicity genes. The importance of arginine metabolism has been reported in multiple pathogens like Salmonella typhimurium, Helicobacter pylori, Streptococcus pneumoniae, Pseudomonas aeruginosa, and Mycobacterium tuberculosis as a source of energy and as a trigger for polyamine synthesis required for efficient pathogenesis. Owing to the critical role of arginine in establishing pathogenesis, several pathogens employ an array of mechanisms for finetuning arginine metabolism [115], and breach of this finetuning can be expected to compromise bacterial fitness. While pathogens employ strategies to counteract immune responses by interfering with host arginine metabolism, our study shows Silversol to perform the same against S. aureus. However, Silversol's growth-inhibitory action against other pathogens may or may not stem from the same mode of action. For example, in our recent study [37] describing Silversol's anti-P. aeruginosa activity, arginine metabolism was not found to be among the physiological traits attacked by this colloidal silver formulation. Pharmaceutics **2024**, 16, 726 21 of 27

It is possible that despite being a broad-spectrum antibacterial agent, the mode of action of Silversol against different pathogenic bacteria may differ more or less.

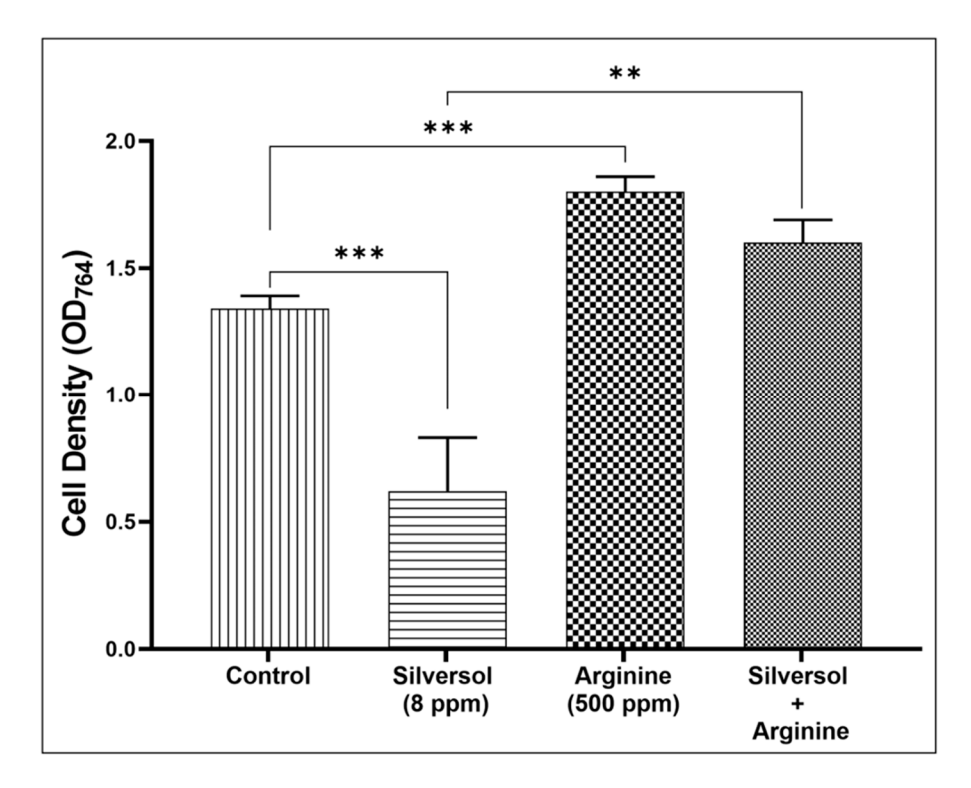


Figure 7. *S. aureus* can resist Silversol's growth-inhibitory effect in the presence of arginine. When *S. aureus* was challenged with Silversol (sub-MIC) in the absence or presence of arginine, in the latter case Silversol did not demonstrate its antibacterial effect. However, this protection against Silversol conferred on bacteria by arginine-supplementation of media disappeared when a higher concentration of Silversol was used to challenge *S. aureus*. It is possible that at higher concentrations the bactericidal effect of Silversol might stem from additional modes of action, rather than inhibiting arginine biosynthesis ** $p \le 0.01$, *** $p \le 0.001$.

A gene co-occurrence pattern analysis of gene families across genomes (via STRING) was also conducted with respect to the two potential hubs identified by us and confirmed using PCR (Figure 6A). These two genes appeared to have homologues in a few other important pathogens too (Figure 6B), particularly *Streptococcus pneumoniae*. Whether Silversol's antibacterial action against other pathogenic bacteria also involves targeting arginine biosynthesis remains an interesting question to be pursued.

4. Conclusions

This study investigated the antibacterial effect of the colloidal nanosilver formulation, Silversol, against antibiotic-resistant *S. aureus*. Silversol could exert its antibacterial effect at ppm-level concentration, while it has been shown to be non-toxic at even higher concentrations for cell lines, animals, and humans. A summary of various studies on the safety of Silversol for human use can be read in [23]. This formulation was found to inhibit the growth of *S. aureus* by targeting a wide variety of genes and physiological traits including efflux, biofilm and exopolysaccharide formation, antibiotic susceptibility, arginine biosynthesis, protein synthesis, potassium uptake, transcriptional regulators, etc. A summary of multiple modes of action of Silversol against *S. aureus* is presented in Figure 8. Particularly, arginine metabolism appeared to be one of the major targets of Silversol in *S. aureus*. While aromatic amino acid biosynthesis has been shown as a viable target in *S. aureus* [117], and *argJ* was shown to be a potential core regulator for *S. aureus* persistence in various stresses [94]; to the best of our knowledge, this is the first report showing *argG* and *argH* as important

Pharmaceutics **2024**, 16, 726 22 of 27

antibacterial targets in this pathogen. Though the antibacterial mechanisms of silver and its nanoformulations have been investigated extensively over the past decades, arginine biosynthesis was hitherto not shown to be targeted by silver in susceptible bacteria. Greater insights into the arginine metabolism of pathogenic bacteria and the relationship of arginine metabolism with bacterial pathogenesis would provide possible targets for controlling bacterial infections. Arginine-tagged drug delivery systems can be designed to target specific subcellular locations like pathogen-containing vacuoles inside host cells. In view of the rampant antibiotic resistance, targeting arginine biosynthesis in bacterial pathogens may be a potent approach toward the development of next-generation anti-pathogenic formulations. Important targets in *S. aureus* attacked by Silversol identified in this study can prove vital input for other antibacterial drug discovery programs. Amino acid biosynthesis pathways are critical for bacterial growth in nutrient-limiting conditions in the host. Surprising connections between bacterial nutrient biosynthesis and antibiotic resistance have been revealed recently [118]. These idiosyncratic connections offer an untapped opportunity for designing novel approaches to combat antibiotic-resistant pathogens.

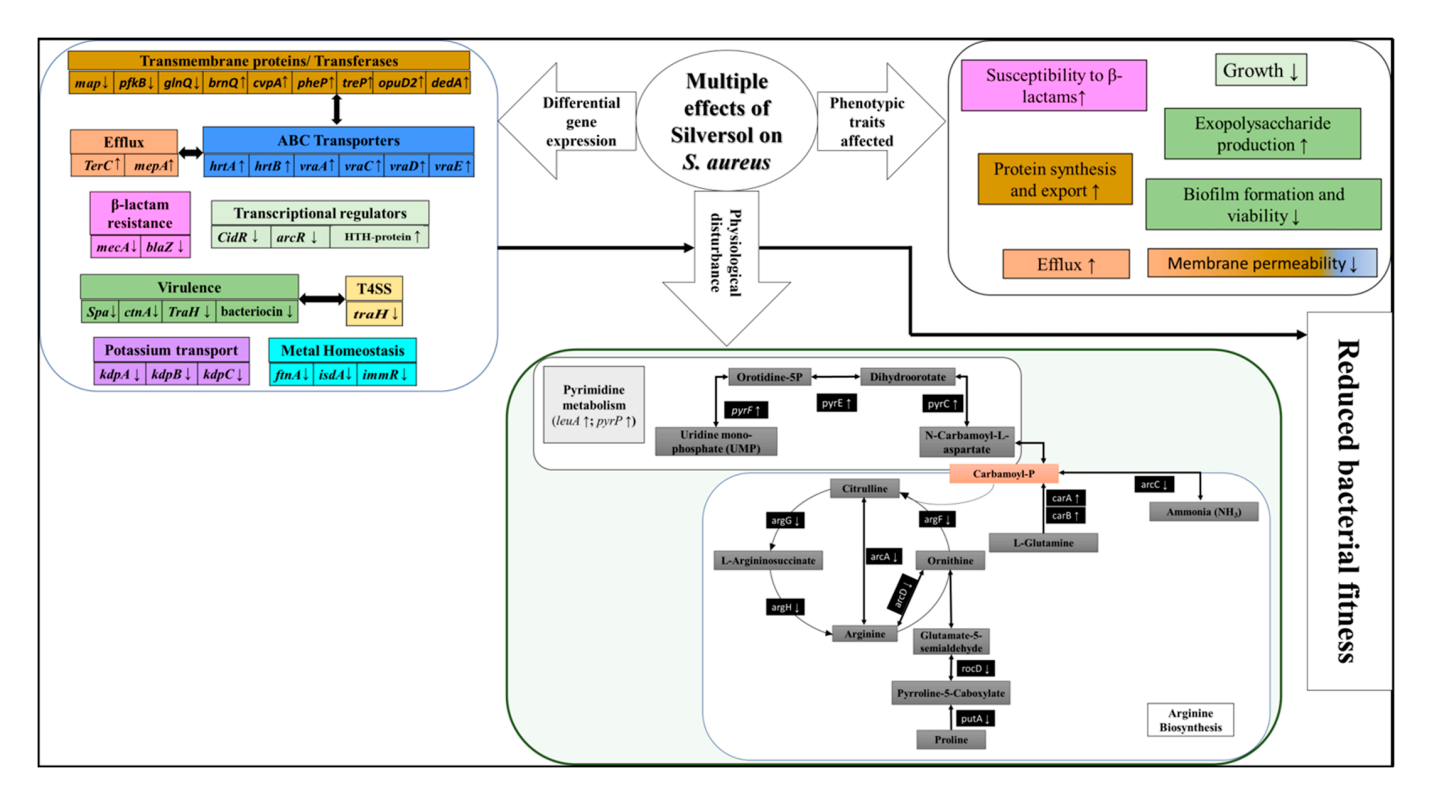


Figure 8. A schematic summary of multiple effects of Silversol on *S. aureus*. Different physiological and phenotypic traits of *S. aureus* affected under the influence of sub-lethal levels of Silversol are shown. Boxes with identical colors have mutual functional relevance. (\uparrow) or (\downarrow) arrow indicates the up- or down-regulation of the concerned gene.

Supplementary Materials: The following supporting information can be downloaded at: https://www.mdpi.com/article/10.3390/pharmaceutics16060726/s1, Figure S1: Antibiogram of S. aureus generated through Kirby-Bauer Disc Diffusion assay; Figure S2. Antibiotic-resistant strain of *S. aureus* used in our study could kill all the host worms within 24 h; Figure S3. A schematic presentation of the methodology/workflow employed for whole transcriptome and network analysis; Figure S4. Silversol's antibacterial effect against *S. aureus* does not follow a strictly linear dose-response pattern; Figure S5. Bacteriostatic and bactericidal effect of Silversol®against *S. aureus* at low and high concentrations respectively; Figure S6. Heat map of DEGs in Silversol®-exposed *S. aureus*; Figure S7. Volcano Plot of experimental versus control samples. Table S1. Antibiogram of antibiotic-resistant *Staphylococcus aureus* generated through Kirby-Bauer Disc Diffusion assay; Table S2. Quantification of extracted RNA, library, and insert size; Table S3. Temperature profile for RT-PCR assay.

Author Contributions: Conceptualization: D.M. and V.K.; methodology: G.G., N.T. and V.K.; formal analysis, investigation, data curation: N.T. and G.G.; resources: D.M. and V.K.; writing—original draft preparation: G.G., N.T. and V.K.; writing—review and editing: N.T., G.G., D.M. and V.K.; supervision and project administration: V.K.; funding acquisition: D.M. and V.K. All authors have read and agreed to the published version of the manuscript.

Funding: This study received no extramural financial support.

Institutional Review Board Statement: Not applicable.

Informed Consent Statement: Not applicable.

Data Availability Statement: All the data are included within the main manuscript or Supplementary Materials.

Acknowledgments: We thank NERF (Nirma Education and Research Foundation), Ahmedabad, for infrastructural support, and for providing a doctoral stipend to N.T. and G.G. acknowledges a scholarship from the Government of Gujarat via their SHODH scheme. Anselm DeSouza and Chhaya Godse from Viridis Biopharma are thanked for the pre-submission review of the manuscript.

Conflicts of Interest: D.M. is affiliated with Viridis Biopharma Pvt. Ltd., which manufactures and markets Silversol[®]. However, this in no way has influenced the design of the study or the interpretation of results. The rest of the authors declare no competing interests.

References

- 1. Saper, R.B.; Kales, S.N.; Paquin, J.; Burns, M.J.; Eisenberg, D.M.; Davis, R.B.; Phillips, R.S. Heavy metal content of ayurvedic herbal medicine products. *JAMA* **2004**, 292, 2868–2873. [CrossRef]
- 2. Inder, D.; Kumar, P. Sedative-hypnotic effect of ash of silver in mice: A reverse pharmacological study. *J. Tradit. Complement. Med.* **2014**, *4*, 268–271. [CrossRef]
- 3. Parimalam, S.S.; Sohrabi, A.; Badilescu, S.; Bhat, R.; Piekny, A.; Packirisamy, M. Study of Incinerated Silver Used in Indian Traditional Medicine Systems. *Int. J. Theor. Appl. Nanotechnol.* **2020**, 1929, 1248. [CrossRef]
- 4. Burange, P.J.; Tawar, M.G.; Bairagi, R.A.; Malviya, V.R.; Sahu, V.K.; Shewatkar, S.N.; Sawarkar, R.A.; Mamurkar, R.R. Synthesis of silver nanoparticles by using Aloe vera and Thuja orientalis leaves extract and their biological activity: A comprehensive review. *Bull. Natl. Res. Cent.* **2021**, 45, 181. [CrossRef]
- 5. Korkmaz, N. Bioreduction: The biological activity, characterization, and synthesis of silver nanoparticles. *Turk. J. Chem.* **2020**, *44*, 325–334. [CrossRef]
- 6. Khan, M.; Khan, T.; Wahab, S.; Aasim, M.; Sherazi, T.A.; Zahoor, M.; Yun, S.I. Solvent based fractional biosynthesis, phytochemical analysis, and biological activity of silver nanoparticles obtained from the extract of *Salvia moorcroftiana*. *PLoS ONE* **2023**, *18*, e0287080. [CrossRef]
- 7. Balasubramaniam, B.; Prateek Ranjan, S.; Saraf, M.; Kar, P.; Singh, S.P.; Thakur, V.K.; Singh, A.; Gupta, R.K. Antibacterial and antiviral functional materials: Chemistry and biological activity toward tackling COVID-19-like pandemics. *ACS Pharmacol. Transl. Sci.* 2020, 4, 8–54. [CrossRef]
- 8. Jain, N.; Jain, P.; Rajput, D.; Patil, U.K. Green synthesized plant-based silver nanoparticles: Therapeutic prospective for anticancer and antiviral activity. *Micro Nano Syst. Lett.* **2021**, *9*, 5. [CrossRef]
- 9. Ratan, Z.A.; Mashrur, F.R.; Chhoan, A.P.; Shahriar, S.M.; Haidere, M.F.; Runa, N.J.; Kim, S.; Kweon, D.H.; Hosseinzadeh, H.; Cho, J.Y. Silver nanoparticles as potential antiviral agents. *Pharmaceutics* **2021**, *13*, 2034. [CrossRef]
- 10. Ibrahim, O.M.; Abed, A.M.; Yahea, N.Z. Evaluation of biological activity of greenly synthesized silver nanoparticles using aloe vera gel extract as antibacterial agent in-vitro and in-vivo. *Iraqi J. Agric. Sci.* **2020**, *51*, 1706–1715.
- 11. Bruna, T.; Maldonado-Bravo, F.; Jara, P.; Caro, N. Silver nanoparticles and their antibacterial applications. *Int. J. Mol. Sci.* **2021**, 22, 7202. [CrossRef]
- 12. Mussin, J.; Giusiano, G. Biogenic silver nanoparticles as antifungal agents. Front. Chem. 2022, 10, 1023542. [CrossRef]
- 13. Matras, E.; Gorczyca, A.; Przemieniecki, S.W.; Oćwieja, M. Surface properties-dependent antifungal activity of silver nanoparticles. *Sci. Rep.* **2022**, *12*, 18046. [CrossRef]
- 14. Abou Elez, R.M.; Attia, A.S.; Tolba, H.M.; Anter, R.G.; Elsohaby, I. Molecular identification and antiprotozoal activity of silver nanoparticles on viability of Cryptosporidium parvum isolated from pigeons, pigeon fanciers and water. *Sci. Rep.* **2023**, *13*, 3109. [CrossRef]
- 15. Majumdar, R.; Kar, P.K. Biosynthesis, characterization and anthelmintic activity of silver nanoparticles of *Clerodendrum infortuna-tum* isolate. *Sci. Rep.* **2023**, *13*, 7415. [CrossRef]
- 16. Gajera, G.; Godse, C.; DeSouza, A.; Mehta, D.; Kothari, V. Potent anthelmintic activity of a colloidal nano-silver formulation (Silversol®) against the model worm *Caenorhabditis elegans*. *BMC Res. Notes* **2023**, *16*, 130. [CrossRef]
- 17. Wu, K.; Li, H.; Cui, X.; Feng, R.; Chen, W.; Jiang, Y.; Tang, C.; Wang, Y.; Wang, Y.; Shen, X.; et al. Mutagenesis and resistance development of bacteria challenged by silver nanoparticles. *Antimicrob. Agents Chemother.* **2022**, *66*, e00628-22. [CrossRef]

18. Ahmad, A.; Wei, Y.; Syed, F.; Tahir, K.; Rehman, A.U.; Khan, A.; Ullah, S.; Yuan, Q. The effects of bacteria-nanoparticles interface on the antibacterial activity of green synthesized silver nanoparticles. *Microb. Pathog.* **2017**, *102*, 133–142. [CrossRef]

- 19. Mazur, P.; Skiba-Kurek, I.; Mrowiec, P.; Karczewska, E.; Drożdż, R. Synergistic ROS-associated antimicrobial activity of silver nanoparticles and gentamicin against staphylococcus epidermidis. *Int. J. Nanomed.* **2020**, *15*, 3551–3562. [CrossRef]
- 20. Reeves, C.M.; Magallon, J.; Rocha, K.; Tran, T.; Phan, K.; Vu, P.; Yi, Y.; Oakley-Havens, C.L.; Cedano, J.; Jimenez, V.; et al. Aminoglycoside 6'-N-acetyltransferase Type Ib [AAC(6')-Ib]-Mediated Aminoglycoside Resistance: Phenotypic Conversion to Susceptibility by Silver Ions. *Antibiotics* **2020**, *10*, 29. [CrossRef]
- 21. Yin, I.X.; Zhang, J.; Zhao, I.S.; Mei, M.L.; Li, Q.; Chu, C.H. The antibacterial mechanism of silver nanoparticles and its application in dentistry. *Int. J. Nanomed.* **2020**, *17*, 2555–2562. [CrossRef]
- 22. Jiang, S.; Wang, F.; Cao, X.; Slater, B.; Wang, R.; Sun, H.; Wang, H.; Shen, X.; Yao, Z. Novel application of ion exchange membranes for preparing effective silver and copper based antibacterial membranes. *Chemosphere* **2022**, 287, 132131. [CrossRef]
- 23. De Souza, A.; Vora, A.H.; Mehta, A.D.; Moeller, K.; Moeller, C.; Willoughby, A.J.; Godse, C.S. SilverSol[®] a Nano-Silver Preparation: A Multidimensional Approach to Advanced Wound Healing. In *Wound Healing Research*; Kumar, P., Kothari, V., Eds.; Springer: Singapore, 2021; pp. 355–396. [CrossRef]
- 24. Khan, S.A.; Johnson, M.E.; Kalan, M.S.; Montoro Bustos, A.R.; Rabb, S.A.; Strenge, I.H.; Murphy, K.E.; Croley, T.R. Characterization of nanoparticles in silicon dioxide food additive. *Food Addit. Contam. Part A* **2024**, *41*, 9–21. [CrossRef]
- 25. Abbasi, R.; Shineh, G.; Mobaraki, M.; Doughty, S.; Tayebi, L. Structural parameters of nanoparticles affecting their toxicity for biomedical applications: A review. *J. Nanopart. Res.* **2023**, 25, 43. [CrossRef]
- 26. Saha, S.; Ali, M.R.; Khaleque, M.A.; Bacchu, M.S.; Aly, M.A.; Khan, M.Z. Metal oxide nanocarrier for targeted drug delivery towards the treatment of global infectious diseases: A review. *J. Drug Deliv. Sci. Technol.* **2023**, *86*, 104728. [CrossRef]
- 27. Nikolova, M.P.; Chavali, M.S. Metal oxide nanoparticles as biomedical materials. Biomimetics 2020, 5, 27. [CrossRef]
- 28. Weiner, L.M.; Webb, A.K.; Limbago, B.; Dudeck, M.A.; Patel, J.; Kallen, A.J.; Edwards, J.R.; Sievert, D.M. Antimicrobial-resistant pathogens associated with healthcare-associated infections: Summary of data reported to the National Healthcare Safety Network at the Centers for Disease Control and Prevention, 2011–2014. *Infect. Control Hosp. Epidemiol.* 2016, 37, 1288–1301. [CrossRef]
- 29. Tran, P.L.; Luth, K.; Wang, J.; Ray, C.; de Souza, A.; Mehta, D.; Moeller, K.W.; Moeller, C.D.; Reid, T.W. Efficacy of a silver colloidal gel against selected oral bacteria in vitro. F1000Research 2019, 8, 267. [CrossRef]
- 30. Ludwig, N.; Thörner-van Almsick, J.; Mersmann, S.; Bardel, B.; Niemann, S.; Chasan, A.I.; Schäfers, M.; Margraf, A.; Rossaint, J.; Kahl, B.C.; et al. Nuclease activity and protein A release of *Staphylococcus aureus* clinical isolates determine the virulence in a murine model of acute lung infection. *Front. Immunol.* 2023, 14, 1259004. [CrossRef]
- 31. Kharat, A.S.; Makwana, N.; Nasser, M.; Gayen, S.; Yadav, B.; Kumar, D.; Veeraraghavan, B.; Mercier, C. Dramatic increase in antimicrobial resistance in ESKAPE clinical isolates over the 2010-2020 decade in India. *Int. J. Antimicrob. Agents* **2024**, *63*, 107125. [CrossRef]
- 32. EUCAST Guidelines for Detection of Resistance Mechanisms and Specific Resistances of Clinical and/or Epidemiological Importance 2017. Version 2.0. Available online: https://aurosan.de/images/mediathek/servicematerial/EUCAST_detection_of_resistance_mechanisms.pdf (accessed on 25 April 2024).
- 33. Turnidge, J.D. Susceptibility test methods: General considerations. Man. Clin. Microbiol. 2015, 25, 1246–1252.
- 34. Ramadan, M.A.; Tawfik, A.F.; Shibl, A.M.; Gemmell, C.G. Post-antibiotic effect of azithromycin and erythromycin on streptococcal susceptibility to phagocytosis. *J. Med. Microbiol.* **1995**, 42, 362–366. [CrossRef]
- 35. Pfaller, M.A.; Sheehan, D.J.; Rex, J.H. Determination of fungicidal activities against yeasts and molds: Lessons learned from bactericidal testing and the need for standardization. *Clin. Microbiol. Rev.* **2004**, *17*, 268–280. [CrossRef]
- 36. Simner, P.J.; Hindler, J.A.; Bhowmick, T.; Das, S.; Johnson, J.K.; Lubers, B.V.; Redell, M.A.; Stelling, J.; Erdman, S.M. What's New in Antibiograms? Updating CLSI M39 Guidance with current trends. *J. Clin. Microbiol.* **2022**, *60*, e02210-21. [CrossRef]
- 37. Gajera, G.; Thakkar, N.; Godse, C.; DeSouza, A.; Mehta, D.; Kothari, V. Sub-lethal concentration of a colloidal nanosilver formulation (Silversol®) triggers dysregulation of iron homeostasis and nitrogen metabolism in multidrug resistant Pseudomonas aeruginosa. *BMC Microbiol.* **2023**, 23, 303. [CrossRef]
- 38. Hirshfield, I.; Barua, S.; Basu, P. Overview of biofilms and some key methods for their study. In *Practical Handbook of Microbiology*, 2nd ed.; Goldman, E., Green, L.H., Eds.; CRC Press: Boca Raton, FL, USA, 2009; pp. 675–688, Chapter 42.
- 39. Trafny, E.A.; Lewandowski, R.; Zawistowska-Marciniak, I.; Stępińska, M. Use of MTT assay for determination of the biofilm formation capacity of microorganisms in metalworking fluids. *World J. Microbiol. Biotechnol.* **2013**, 29, 1635–1643. [CrossRef]
- 40. Andhare, P.; Goswami, D.; Delattre, C.; Pierre, G.; Michaud, P.; Pathak, H. Edifying the strategy for the finest extraction of succinoglycan from *Rhizobium radiobacter* strain CAS. *Appl. Biol. Chem.* **2017**, *60*, 339–348. [CrossRef]
- 41. Mullin, S.; Mani, N.; Grossman, T.H. Inhibition of antibiotic efflux in bacteria by the novel multidrug resistance inhibitors biricodar (VX-710) and timcodar (VX-853). *Antimicrob. Agents Chemother.* **2004**, *48*, 4171–4176. [CrossRef]
- 42. Lowry, O.H.; Rosebrough, N.J.; Farr, A.L.; Randall, R.J. Protein measurement with the Folin phenol reagent. *J. Biol. Chem.* **1951**, 193, 265–275. [CrossRef]
- 43. Dulley, J.R.; Grieve, P.A. A simple technique for eliminating interference by detergents in the Lowry method of protein determination. *Anal. Biochem.* **1975**, *64*, 136–141. [CrossRef]
- 44. Mishra, M.; Tiwari, S.; Gomes, A.V. Protein purification and analysis: Next generation Western blotting techniques. *Expert Rev. Proteom.* **2017**, *14*, 1037–1053. [CrossRef] [PubMed]

Pharmaceutics **2024**, 16, 726 25 of 27

45. Crowley, L.C.; Scott, A.P.; Marfell, B.J.; Boughaba, J.A.; Chojnowski, G.; Waterhouse, N.J. Measuring cell death by propidium iodide uptake and flow cytometry. *Cold Spring Harb. Protoc.* **2016**, 2016, pdb-rot087163. [CrossRef] [PubMed]

- 46. Mombeshora, M.; Mukanganyama, S. Antibacterial activities, proposed mode of action and cytotoxicity of leaf extracts from *Triumfetta welwitschii* against *Pseudomonas aeruginosa*. *BMC Complement*. *Altern*. *Med.* **2019**, 19, 315. [CrossRef] [PubMed]
- 47. Andrews, S. FastQC: A Quality Control Tool for High Throughput Sequence Data. 2010. Available online: https://www.bioinformatics.babraham.ac.uk/projects/fastqc/ (accessed on 1 May 2024).
- 48. Chen, S.; Zhou, Y.; Chen, Y.; Gu, J. fastp: An ultra-fast all-in-one FASTQ preprocessor. *Bioinformatics* **2018**, 34, i884-90. [CrossRef] [PubMed]
- 49. Langmead, B.; Salzberg, S.L. Fast gapped-read alignment with Bowtie 2. Nat. Methods 2012, 9, 357–359. [CrossRef] [PubMed]
- 50. Liao, Y.; Smyth, G.K.; Shi, W. featureCounts: An efficient general purpose program for assigning sequence reads to genomic features. *Bioinformatics* **2014**, *30*, 923–930. [CrossRef] [PubMed]
- 51. Robinson, M.D.; McCarthy, D.J.; Smyth, G.K. edgeR: A Bioconductor package for differential expression analysis of digital gene expression data. *Bioinformatics* **2010**, *26*, 139–140. [CrossRef] [PubMed]
- 52. Conesa, A.; Götz, S. Blast2GO: A comprehensive suite for functional analysis in plant genomics. *Int. J. Plant Genom.* **2008**, 2008, 619832. [CrossRef] [PubMed]
- 53. Ye, J.; Zhang, Y.; Cui, H.; Liu, J.; Wu, Y.; Cheng, Y.; Xu, H.; Huang, X.; Li, S.; Zhou, A.; et al. WEGO 2.0: A web tool for analyzing and plotting GO annotations, 2018 update. *Nucleic Acids Reserach* 2018, 46, W71–W75. [CrossRef] [PubMed]
- 54. Szklarczyk, D.; Gable, A.L.; Lyon, D.; Junge, A.; Wyder, S.; Huerta-Cepas, J.; Simonovic, M.; Doncheva, N.T.; Morris, J.H.; Bork, P.; et al. STRING v11: Protein–protein association networks with increased coverage, supporting functional discovery in genome-wide experimental datasets. *Nucleic Acids Research* 2019, 47, D607-13. [CrossRef] [PubMed]
- 55. Chin, C.H.; Chen, S.H.; Wu, H.H.; Ho, C.W.; Ko, M.T.; Lin, C.Y. cytoHubba: Identifying hub objects and sub-networks from complex interactome. *BMC Syst. Biol.* **2014**, *8*, S11. [CrossRef] [PubMed]
- 56. Shannon, P.; Markiel, A.; Ozier, O.; Baliga, N.S.; Wang, J.T.; Ramage, D.; Amin, N.; Schwikowski, B.; Ideker, T. Cytoscape: A software environment for integrated models of biomolecular interaction networks. *Genome Res.* **2003**, *13*, 2498–2504. [CrossRef] [PubMed]
- 57. Untergasser, A.; Nijveen, H.; Rao, X.; Bisseling, T.; Geurts, R.; Leunissen, J.A. Primer3Plus, an enhanced web interface to Primer3. *Nucleic Acids Res.* **2007**, *35* (Suppl. S2), W71–W74. [CrossRef] [PubMed]
- 58. Calabrese, E.J. Hormesis: A revolution in toxicology, risk assessment and medicine: Re-framing the dose–response relationship. *EMBO Rep.* **2004**, *5*, S37–S40. [CrossRef] [PubMed]
- 59. Iavicoli, I.; Fontana, L.; Agathokleous, E.; Santocono, C.; Russo, F.; Vetrani, I.; Fedele, M.; Calabrese, E.J. Hormetic dose responses induced by antibiotics in bacteria: A phantom menace to be thoroughly evaluated to address the environmental risk and tackle the antibiotic resistance phenomenon. *Sci. Total Environ.* **2021**, *798*, 149255. [CrossRef] [PubMed]
- Eagle, H.; Musselman, A.D. The rate of bactericidal action of penicillin in vitro as a function of its concentration, and its paradoxically reduced activity at high concentrations against certain organisms. J. Exp. Med. 1948, 88, 99–131. [CrossRef] [PubMed]
- 61. Shah, P.M.; Troche, G.; Stille, W. Effect of concentration on bactericidal activity of cefotaxime. *J. Antimicrob. Chemother.* **1979**, *5*, 419–422. [CrossRef] [PubMed]
- 62. Eagle, H. The recovery of bacteria from the toxic effects of penicillin. J. Clin. Investig. 1949, 28, 832–836. [CrossRef]
- 63. Eagle, H.; Fleischman, R.; Musselman, A.D. The bactericidal action of penicillin in vivo: The participation of the host, and the slow recovery of the surviving organisms. *Ann. Intern. Med.* **1950**, *33*, 544–571. [CrossRef] [PubMed]
- 64. Stille, W.; Uffelmann, H. Untersuchung über den paradoxen bakteriziden Effekt von Penicillinen auf Enterokokken (Eagle-Effekt). DMW Dtsch. Med. Wochenschr. 1973, 98, 611–613. [CrossRef] [PubMed]
- 65. Yourassowsky, E.; Vanderlinden, M.P.; Schoutens, E. A rapid, simple method for demonstrating synergy of amikacin and penicillin against various microorganisms. *J. Infect. Dis.* **1976**, 134 (Suppl. S2), S275–S279. [CrossRef] [PubMed]
- 66. Kerry, D.W.; Hamilton-Miller, J.M.; Brumfitt, W. Paradoxical effect of mecillinam on *Providencia sfuaríii*. *J. Antimicrob. Chemother.* **1976**, 2, 368–388. [CrossRef] [PubMed]
- 67. Lorian, V.; Silletti, R.P.; Biondo, F.X.; De Freitas, C.C. Paradoxical effect of aminoglycoside antibiotics on the growth of Gramnegative bacilli. *J. Antimicrob. Chemother.* **1979**, *5*, 613–616. [CrossRef] [PubMed]
- 68. Fuda, C.C.; Fisher, J.F.; Mobashery, S. β-Lactam resistance in *Staphylococcus aureus*: The adaptive resistance of a plastic genome. *Cell. Mol. Life Sci.* **2005**, *62*, 2617–2633. [CrossRef] [PubMed]
- 69. Zhao, A.; Sun, J.; Liu, Y. Understanding bacterial biofilms: From definition to treatment strategies. *Front. Cell. Infect. Microbiol.* **2023**, *13*, 1137947. [CrossRef] [PubMed]
- 70. Mishra, S.; Gupta, A.; Upadhye, V.; Singh, S.C.; Sinha, R.P.; Häder, D.P. Therapeutic strategies against biofilm infections. *Life* **2023**, 13, 172. [CrossRef] [PubMed]
- 71. Diban, F.; Di Lodovico, S.; Di Fermo, P.; D'Ercole, S.; D'Arcangelo, S.; Di Giulio, M.; Cellini, L. Biofilms in chronic wound infections: Innovative antimicrobial approaches using the in vitro Lubbock chronic wound biofilm model. *Int. J. Mol. Sci.* 2023, 24, 1004. [CrossRef] [PubMed]
- 72. Flemming, H.C. EPS—Then and now. Microorganisms 2016, 4, 41. [CrossRef] [PubMed]

Pharmaceutics **2024**, 16, 726 26 of 27

73. Wang, X.; Liu, M.; Yu, C.; Li, J.; Zhou, X. Biofilm formation: Mechanistic insights and therapeutic targets. *Mol. Biomed.* **2023**, *4*, 49. [CrossRef] [PubMed]

- 74. Mielnichuk, N.; Joya, C.M.; Monachesi, M.A.; Bertani, R.P. Exopolysaccharide Production and Precipitation Method as a Tool to Study Virulence Factors. In *Host-Pathogen Interactions: Methods and Protocols*; Springer US: New York, NY, USA, 2024; pp. 71–79.
- 75. Wang, J.; Li, G.; Yin, H.; An, T. Bacterial response mechanism during biofilm growth on different metal material substrates: EPS characteristics, oxidative stress and molecular regulatory network analysis. *Environ. Res.* **2020**, *185*, 109451. [CrossRef] [PubMed]
- 76. Chen, M.; Cai, Y.; Li, G.; Zhao, H.; An, T. The stress response mechanisms of biofilm formation under sub-lethal photocatalysis. *Appl. Catal. B Environ.* **2022**, *307*, 121200. [CrossRef]
- 77. Sun, J.; Deng, Z.; Yan, A. Bacterial multidrug efflux pumps: Mechanisms, physiology and pharmacological exploitations. *Biochem. Biophys. Res. Commun.* **2014**, 453, 254–267. [CrossRef] [PubMed]
- 78. Brown, M.H.; Skurray, R.A. Staphylococcal multidrug efflux protein QacA. J. Mol. Microbiol. Biotechnol. 2001, 3, 163–170. [PubMed]
- 79. Pagès, J.M.; Masi, M.; Barbe, J. Inhibitors of efflux pumps in Gram-negative bacteria. *Trends Mol. Med.* **2005**, *11*, 382–389. [CrossRef] [PubMed]
- 80. Lennen, R.M.; Politz, M.G.; Kruziki, M.A.; Pfleger, B.F. Identification of transport proteins involved in free fatty acid efflux in *Escherichia coli*. *J. Bacteriol*. **2013**, 195, 135–144. [CrossRef] [PubMed]
- 81. Singh, V.K.; Jayaswal, R.K.; Wilkinson, B.J. Cell wall-active antibiotic induced proteins of *Staphylococcus aureus* identified using a proteomic approach. *FEMS Microbiol. Lett.* **2001**, 199, 79–84. [CrossRef] [PubMed]
- 82. Liu, B.; Qian, S.B. Translational reprogramming in cellular stress response. *Wiley Interdiscip. Rev. RNA* **2014**, *5*, 301–305. [CrossRef] [PubMed]
- 83. Nikolic, P.; Mudgil, P. The cell wall, cell membrane and virulence factors of *Staphylococcus aureus* and their role in antibiotic resistance. *Microorganisms* **2023**, *11*, 259. [CrossRef] [PubMed]
- 84. Olchowik-Grabarek, E.; Sękowski, S.; Kwiatek, A.; Płaczkiewicz, J.; Abdulladjanova, N.; Shlyonsky, V.; Swiecicka, I.; Zamaraeva, M. The structural changes in the membranes of *Staphylococcus aureus* caused by hydrolysable tannins witness their antibacterial activity. *Membranes* 2022, 12, 1124. [CrossRef] [PubMed]
- 85. Chaudhari, S.S.; Thomas, V.C.; Sadykov, M.R.; Bose, J.L.; Ahn, D.J.; Zimmerman, M.C.; Bayles, K.W. The LysR-type transcriptional regulator, CidR, regulates stationary phase cell death in *Staphylococcus aureus*. *Mol. Microbiol.* **2016**, *101*, 942–953. [CrossRef] [PubMed]
- 86. Yang, S.J.; Rice, K.C.; Brown, R.J.; Patton, T.G.; Liou, L.E.; Park, Y.H.; Bayles, K.W. A LysR-type regulator, CidR, is required for induction of the *Staphylococcus aureus* cidABC operon. *J. Bacteriol.* **2005**, *187*, 5893–5900. [CrossRef] [PubMed]
- 87. Rigi, G.; Ghaedmohammadi, S.; Ahmadian, G. A comprehensive review on staphylococcal protein A (SpA): Its production and applications. *Biotechnol. Appl. Biochem.* **2019**, *66*, 454–464. [CrossRef] [PubMed]
- 88. Merino, N.; Toledo-Arana, A.; Vergara-Irigaray, M.; Valle, J.; Solano, C.; Calvo, E.; Lopez, J.A.; Foster, T.J.; Penadés, J.R.; Lasa, I. Protein A-mediated multicellular behavior in *Staphylococcus aureus*. *J. Bacteriol.* **2009**, 191, 832–843. [CrossRef] [PubMed]
- 89. Remy, L.; Carrière, M.; Derré-Bobillot, A.; Martini, C.; Sanguinetti, M.; Borezée-Durant, E. The *Staphylococcus aureus* Opp1 ABC transporter imports nickel and cobalt in zinc-depleted conditions and contributes to virulence. *Mol. Microbiol.* **2013**, *87*, 730–743. [CrossRef] [PubMed]
- 90. Rutherford, J.C. The emerging role of urease as a general microbial virulence factor. *PLoS Pathog.* **2014**, *10*, e1004062. [CrossRef] [PubMed]
- 91. Aliyeva-Schnorr, L.; Schuster, C.; Deising, H.B. Natural urease inhibitors reduce the severity of disease symptoms, dependent on the lifestyle of the pathogens. *J. Fungi* **2023**, *9*, 708. [CrossRef] [PubMed]
- 92. Oliyaei, N.; Hashempur, M.H.; Zomorodian, K.; Tanideh, N.; Noori, M.; Abbasi, A.; Mahdavi, M.; Iraji, A. An overview of potential algae-derived bioactive compounds against urease-positive microorganisms. *Algal Res.* **2023**, *77*, 103372. [CrossRef]
- 93. Laverde, D.; Probst, I.; Romero-Saavedra, F.; Kropec, A.; Wobser, D.; Keller, W.; Grohmann, E.; Huebner, J. Targeting type IV secretion system proteins to combat multidrug-resistant Gram-positive pathogens. *J. Infect. Dis.* **2017**, 215, 1836–1845. [CrossRef] [PubMed]
- 94. Yee, R.; Feng, J.; Wang, J.; Chen, J.; Zhang, Y. Identification of genes regulating cell death in *Staphylococcus aureus*. *Front. Microbiol.* **2019**, *10*, 480608. [CrossRef] [PubMed]
- 95. Gründling, A. Potassium uptake systems in *Staphylococcus aureus*: New stories about ancient systems. *MBio* **2013**, *4*, 10–128. [CrossRef] [PubMed]
- 96. Xue, T.; You, Y.; Hong, D.; Sun, H.; Sun, B. The *Staphylococcus aureus* KdpDE two-component system couples extracellular K+ sensing and Agr signaling to infection programming. *Infect. Immun.* **2011**, 79, 2154–2167. [CrossRef] [PubMed]
- 97. Guzman, M.; Dille, J.; Godet, S. Synthesis and antibacterial activity of silver nanoparticles against gram-positive and gram-negative bacteria. *Nanomed. Nanotechnol. Biol. Med.* **2012**, *8*, 37–45. [CrossRef] [PubMed]
- 98. Domínguez, A.V.; Algaba, R.A.; Canturri, A.M.; Villodres, Á.R.; Smani, Y. Antibacterial activity of colloidal silver against gram-negative and Gram-positive bacteria. *Antibiotics* **2020**, *9*, 36. [CrossRef] [PubMed]
- 99. Okiki, P.A.; Eromosele, E.S.; Ade-Ojo, P.; Sobajo, O.A.; Idris, O.O.; Agbana, R.D. Occurrence of mecA and blaZ genes in methicillin-resistant *Staphylococcus aureus* associated with vaginitis among pregnant women in Ado-Ekiti, Nigeria. *New Microbes New Infect.* 2020, *38*, 100772. [CrossRef] [PubMed]

Pharmaceutics **2024**, 16, 726 27 of 27

100. Rosato, A.E.; Kreiswirth, B.N.; Craig, W.A.; Eisner, W.; Climo, M.W.; Archer, G.L. mecA-blaZ corepressors in clinical *Staphylococcus aureus* isolates. *Antimicrob. Agents Chemother.* **2003**, 47, 1460–1463. [CrossRef] [PubMed]

- 101. Pereira, L.A.; Harnett, G.B.; Hodge, M.M.; Cattell, J.A.; Speers, D.J. Real-time PCR assay for detection of *blaZ* genes in *Staphylococcus aureus* clinical isolates. *J. Clin. Microbiol.* **2014**, 52, 1259–1261. [CrossRef] [PubMed]
- 102. Attia, A.S.; Benson, M.A.; Stauff, D.L.; Torres, V.J.; Skaar, E.P. Membrane damage elicits an immunomodulatory program in *Staphylococcus aureus*. *PLoS Pathog*. **2010**, *6*, e1000802. [CrossRef] [PubMed]
- 103. Friedman, D.B.; Stauff, D.L.; Pishchany, G.; Whitwell, C.W.; Torres, V.J.; Skaar, E.P. *Staphylococcus aureus* redirects central metabolism to increase iron availability. *PLoS Pathog.* **2006**, 2, e87. [CrossRef] [PubMed]
- 104. Sheldon, J.R.; Laakso, H.A.; Heinrichs, D.E. Iron acquisition strategies of bacterial pathogens. In *Virulence Mechanisms of Bacterial Pathogens*, 5th ed.; John Wiley & Sons, Inc.: Hoboken, NJ, USA, 2016; pp. 43–85. [CrossRef]
- 105. Zughaier, S.M.; Cornelis, P. Role of Iron in bacterial pathogenesis. Front. Cell. Infect. Microbiol. 2018, 8, 344. [CrossRef] [PubMed]
- Ahmad, I.; Nawaz, N.; Dermani, F.K.; Kohlan, A.K.; Saidijam, M.; Patching, S.G. Bacterial multidrug efflux proteins: A major mechanism of antimicrobial resistance. Curr. Drug Targets 2018, 27, 1–3. [CrossRef]
- 107. Paruthiyil, S.; Pinochet-Barros, A.; Huang, X.; Helmann, J.D. Bacillus subtilis TerC family proteins help prevent manganese intoxication. *J. Bacteriol.* **2020**, 202, 10–128. [CrossRef]
- 108. Chen, Q.; Guo, F.; Huang, L.; Wang, M.; Shi, C.; Zhang, S.; Yao, Y.; Wang, M.; Zhu, D.; Jia, R.; et al. Functional characterization of a TerC family protein of *Riemerella anatipestifer* in manganese detoxification and virulence. *Appl. Environ. Microbiol.* **2024**, *90*, e01350-23. [CrossRef] [PubMed]
- 109. Turkovicova, L.; Smidak, R.; Jung, G.; Turna, J.; Lubec, G.; Aradska, J. Proteomic analysis of the TerC interactome: Novel links to tellurite resistance and pathogenicity. *J. Proteom.* **2016**, *136*, 167–173. [CrossRef] [PubMed]
- 110. He, B.; Sachla, A.J.; Helmann, J.D. TerC proteins function during protein secretion to metalate exoenzymes. *Nat. Commun.* **2023**, 14, 6186. [CrossRef] [PubMed]
- 111. Poole, K. Efflux-mediated antimicrobial resistance. J. Antimicrob. Chemother. 2005, 56, 20–51. [CrossRef]
- 112. Kaatz, G.W.; McAleese, F.; Seo, S.M. Multidrug resistance in *Staphylococcus aureus* due to overexpression of a novel multidrug and toxin extrusion (MATE) transport protein. *Antimicrob. Agents Chemother.* **2005**, 49, 1857–1864. [CrossRef]
- 113. Hasani, A.; Madhi, M.; Gholizadeh, P.; Shahbazi Mojarrad, J.; Ahangarzadeh Rezaee, M.; Zarrini, G.; Samadi Kafil, H. Metal nanoparticles and consequences on multi-drug resistant bacteria: Reviving their role. *SN Appl. Sci.* **2019**, *1*, 360. [CrossRef]
- 114. Xiong, L.; Teng, J.L.; Botelho, M.G.; Lo, R.C.; Lau, S.K.; Woo, P.C. Arginine metabolism in bacterial pathogenesis and cancer therapy. *Int. J. Mol. Sci.* **2016**, *17*, 363. [CrossRef]
- 115. Gogoi, M.; Datey, A.; Wilson, K.T.; Chakravortty, D. Dual role of arginine metabolism in establishing pathogenesis. *Curr. Opin. Microbiol.* **2016**, 29, 43–48. [CrossRef] [PubMed]
- 116. Gundlach, J.; Commichau, F.M.; Stülke, J. Perspective of ions and messengers: An intricate link between potassium, glutamate, and cyclic di-AMP. *Curr. Genet.* **2018**, *64*, 191–195. [CrossRef]
- 117. O'Connell, C.; Pattee, P.A.; Foster, T.J. Sequence and mapping of the aroA gene of *Staphylococcus aureus* 8325-4. *Microbiology* **1993**, 139, 1449–1460. [CrossRef]
- 118. Carfrae, L.A.; Brown, E.D. Nutrient stress is a target for new antibiotics. Trends Microbiol. 2023, 31, 571–585. [CrossRef]

Disclaimer/Publisher's Note: The statements, opinions and data contained in all publications are solely those of the individual author(s) and contributor(s) and not of MDPI and/or the editor(s). MDPI and/or the editor(s) disclaim responsibility for any injury to people or property resulting from any ideas, methods, instructions or products referred to in the content.